ADVANCED FUNCTIONAL MATERIALS
www.afm-journal.de

Substrate-Induced and Thin-Film Phases: Polymorphism of Organic Materials on Surfaces

Andrew O. F. Jones, Basab Chattopadhyay, Yves H. Geerts, and Roland Resel**

An increase or modification of structural order in the vicinity of a solid substrate is known for a wide range of materials. For molecular materials crystallizing on a solid surface it has been observed that new polymorphic forms may exist near the interface with the substrate, which have structures different to those observed in the bulk. Such phases are termed as substrate-induced phases (SIPs). The presence of an SIP in a compound or a class of materials can be of crucial significance in terms of their physical properties. However, the factors that drive such a process are not clearly understood or studied in depth. In this feature article, we review the current state of understanding concerning SIPs, giving examples of systems where SIPs have been observed, discussing their origins, and which questions remain to be answered. The role of the substrate in controlling the growth and subsequent structural order has been discussed in detail and the impact of polymorphism on organic electronic device properties has been addressed. Finally, the origin of SIPs has been correlated with their crystal structures and the differences with respect to the bulk structure are highlighted.

1. Introduction

The organization of molecules at an interface with a solid is a common occurrence in nature. While gas molecules do not normally organize at such an interface, the ordering of liquids in the vicinity of a solid wall is well known[1–3] and has implications in the vast number of processes where solid-liquid interfaces present themselves (e.g., during crystal nucleation and growth,[4] heterogeneous catalysis,[5] lubrication,[6] etc.). Ordering arises due to the breaking of the liquid's continuous translational symmetry by the solid wall, leading to a positional ordering of molecules at the interface and a structure different to that of the bulk liquid;[7] order typically exists over a few molecular layers before rapidly decaying to bulk behavior as the distance from the wall increases.[8]

Similar ordering effects can also be observed in the quasiliquids which form on the surface of many solids due to surface melting (also known as premelting):[9,10] the existence of a liquid-like layer a few molecules thick on the surface of a solid below the melting point of the bulk material.[11] The structure within this layer is also found to be different to that of the bulk isotropic liquid,[12] highlighting the ordering occurring at the interface. A converse effect, surface freezing, is also observed in some liquids (primarily *n*-alkanes with $16 \leq n \leq 50$), where a solid monolayer may exist at an interface up to ≈30 °C above the bulk melting point while the rest of the compound is molten.[13–15] Such phase behavior is strongly dependent on molecular shape and has only been observed for chain molecules, which then form layers similar to self-assembled monolayers (SAMs) at the interface with the liquid bulk.[16]

Further examples of molecular ordering at interfaces can be seen in materials which display liquid crystal (LC) phases, a phase behavior also dependent on molecular shape and generally observed for molecules with a highly anisotropic shape (e.g., rod-like, disc-like or bowl-like molecules).[17] LCs have properties of both solids and liquids and display long range order which may be orientational and/or positional; various types of LC phases (mesophases) are possible and normally exist only over a certain temperature range (i.e., they are thermotropic); a further property of LCs is that they generally reach thermodynamic equilibrium in the bulk and at interfaces as a result of their short relaxation time. Nematic (N) phases of calamitic LCs (rod-like molecules with cylindrical symmetry) have no positional order but an orientational order which can be described by a unit vector, *n*, known as the director, which represents the preferred molecular orientation (**Figure 1**, left). A scalar order parameter can also be defined which is related to the average angle the long molecular axes make to the director, *n*.

Increased order is seen in smetic phases (Sm) which have both orientational and positional order; for example in a smetic A phase (SmA) molecules form layers (positional ordering of the molecular mass centers) which are oriented normal to the plane of the layers (orientational order), while smetic C phases (SmC) form layers where molecules are oriented with the long molecular axes tilted at an angle to the molecular layer normal

Dr. A. O. F. Jones, Prof. R. Resel
Institute of Solid State Physics
Graz University of Technology
Petersgasse 16, 8010 Graz, Austria
E-mail: roland.resel@tugraz.at
Dr. B. Chattopadhyay, Prof. Y. H. Geerts
Laboratoire de Chimie des Polymères
Faculté des Sciences
Université Libre de Bruxelles CP206/01
Campus de la Plaine
1050 Brussels, Belgium
E-mail: ygeerts@ulb.ac.be

DOI: 10.1002/adfm.201503169

(Figure 1, center).[17] Surface-induced ordering of nematic LCs on surfaces is a topic which has been well studied, where ordering can be readily achieved on textured surfaces such as rubbed polymers.[18,19] For example, it has been shown that the orientational order of a nematic LC material may differ in the vicinity of the surface when compared to that of the bulk LC,[20] while for the liquid crystalline molecule octylcyanobiphenyl (8CB) a homeotropically aligned smetic phase extending over a few molecular layers is induced at the interface with the substrate while the bulk nematic phase has an orientation determined by the smetic layers and the surface below, i.e., it is anchored to the surface (Figure 1, right).[21–23] 8CB exhibits a phase sequence of Cr $\overset{21.5^{\circ}C}{\longleftrightarrow}$ SmA $\overset{33.5^{\circ}C}{\longleftrightarrow}$ N $\overset{40.5^{\circ}C}{\longleftrightarrow}$ isotropic and also shows positional and orientational order of molecules at an interface with the substrate even at temperatures much higher than the clearing temperature (where the LC transforms to the isotropic state).[24] Tuning of surface properties can also be used to induce specific types of order within LC materials,[25–27] with the type and degree of molecular order potentially strongly effecting the physical properties of a material.[28] As both calamitic and discotic (disc-like) LCs containing conjugated sections may behave as organic semiconductors (OSCs) and have applications in displays and other organic electronic devices,[29,30] understanding the ordering of LCs at interfaces is important for the rational design and future development of devices using LCs.

The structure of crystalline molecular materials at an interface with a solid is also of importance in many fields, e.g. electronics, pharmaceuticals, etc.[31–33] Crystalline materials have a higher degree of order than LCs, with atomic positions ordered within the crystallographic unit cell, which effectively repeats in all directions to form a crystal. The self-organization process of molecules to form crystals is dominated by a combination of close packing considerations and maximizing favorable non-covalent intra- and inter-molecular interactions, with interactions ranging from relatively strong hydrogen bonds to weaker halogen bonds, π–π interactions and van der Waals interactions.[34] When there are multiple ways of satisfying the close packing considerations whilst still producing favorable intra- and intermolecular interactions, different packing arrangements which are very close in energy may be possible and multiple polymorphs may form; the difference in energy between different polymorphs is often < 2 kJ mol^{-1}.[35,36] Different polymorphs have different physical properties (e.g., solubility, morphology, compressibility, etc.) and it is often desirable to isolate the polymorph with the most suitable properties for a given application. The relative thermodynamic stability of different polymorphs is determined by the difference in the Gibbs free energy, G, at a given temperature, T, and constant pressure: $G = H - TS$. The enthalpy term H relates to differences in lattice energy between different polymorphs and the entropy term S is related to the differences in disorder and lattice vibrations between polymorphs.[32] Broadly speaking, two types of polymorphic systems exist: in monotropic systems a single polymorph is always the most thermodynamically stable below the melting point, while in an enantiotropic system the relative stability of different polymorphs changes depending on the temperature. Therefore it follows that, for an enantiotropic system, transitions between polymorphs can be induced by changing the temperature of the system, with one specific polymorph the most thermodynamically stable at a given temperature. However, kinetics can also play a role in determining which polymorph forms and, as crystallization from

Andrew O. F. Jones completed his undergraduate studies in chemistry in 2008 at the University of Glasgow, UK. In 2012, he completed his Ph.D. as an Institut Laue-Langevin (ILL) graduate student, under the guidance of Prof. Chick Wilson and Prof. Garry McIntyre, working at both the ILL in Grenoble, France and at the University of Bath, UK. After a postdoctoral stay at the Université Libre de Bruxelles, Belgium with Prof. Michele Sferrazza, he accepted his current position as a postdoctoral researcher at Graz University of Technology with Prof. Roland Resel. His current research focuses on polymorphism and controlling the structure of organic materials.

Basab Chattopadhyay was born and brought up in the suburbs of Kolkata, India. After obtaining his Master's in Physics in 2005, he completed his PhD in 2011 at Indian Association for the Cultivation of Science (IACS) under the guidance of M. Mukherjee. In 2012 he joined the group of Y. Geerts at the Universitè Libre de Bruxelles (ULB), Belgium as a Marie-Curie International Incoming Fellow. He continues to work in the same group with the mandate of "Chargés de Recherche" awarded in 2015 by FRS-FNRS, Belgium. His current research interests focus on the structural aspects of organic thin films and polymorphism.

Roland Resel was born in the city Drosendorf an der Thaya, Austria. After a master in Physics in 1989, he completed his PhD in 1993 at the Vienna University of Technology. After a post-doctoral fellowship at the University of the Ryukyus, Okinawa, Japan, he started 1995 as research associate at the Graz University of Technology. In the year 2001 he was promoted to an associate professor. His research interest are structural properties of organic thin films for their application in organic electronics.

DOI: 10.1002/adfm.201503169

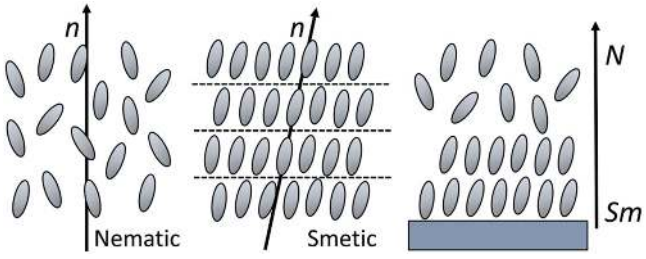

Figure 1. Ordering of different liquid crystalline phases: a nematic (N) phase (left) and smetic (Sm) phase (center) with directors *n* shown; and a liquid crystal with smetic-like ordering at the interface with a solid wall transitioning to nematic ordering in the bulk (right).

solution follows Ostwald's rule of stages (metastable forms nucleate first, before often transforming to more thermodynamically stable polymorphs),[37] it is possible to kinetically trap metastable phases during crystallization by varying the parameters used during crystallization (e.g., choice of solvent,[38] templating using a surface[39,40] or templating in solution).[41]

When molecular materials crystallize on a solid surface, it has been observed that new polymorphic forms may exist near the interface with the substrate which have structures different to those observed in the bulk; the best-known example of such a polymorph is the so-called "thin-film phase" of the prototypical OSC, pentacene.[42] Similar types of polymorphs have been observed for other materials and several terms have been used to describe them including thin-film phases, surface-mediated phases and substrate-induced phases; in this work we will hereafter use the term substrate-induced phase (SIP) to describe these polymorphs. A SIP is defined as a phase with a distinct structure from those of the bulk which occurs in the vicinity of a rigid substrate.

In defining a SIP, it must be stated that SIPs are different to SAMs,[43] as SIPs extend over several molecular layers at least. An SIP is also not necessarily the same as an epitaxially grown film. Epitaxy, traditionally used for inorganic films, is the matching of the crystalline unit cell parameters or geometries of both a substrate and film.[44] It has been developed for organic molecular crystals on crystalline substrates, despite the difficulties arising in creating highly ordered films of molecules with highly anisotropic shapes which often only interact weakly with one another;[45–48] epitaxial growth of organic films on substrates with highly mismatched crystal lattices is also possible.[49,50] Epitaxially grown monolayers may also be used to influence the subsequent film growth on top of them, enabling polymorph selection via epitaxy.[51] SIPs may grow epitaxially,[52] however, they may also occur in the absence of epitaxial effects; SIPs are related specifically to a deviation from the bulk structure in the vicinity of the substrate which is not necessarily related to any matching of unit cells between film and substrate.

As physical properties of materials are strongly correlated with their crystal structures, a divergence from bulk properties near an interface (as is the case when an SIP forms) may have a profound impact on a wide variety of systems. Despite their fundamental importance, SIPs are not well understood and only a small number of systems have been studied in depth. This feature article will cover the current state of understanding concerning SIPs, giving examples of systems where SIPs have been observed, discussing their origins, and which questions remain to be answered. Perhaps the most important questions to be answered are which types of compounds may produce SIPs and the role that the substrate plays in their formation. A particular focus is given to crystalline organic molecular semiconductors, a class of molecules for which the study of SIPs is most advanced; polymers are excluded from the present discussion as they present a large and complex system with different properties to those discussed here and are beyond the scope of this work. The potential impact of SIPs for different fields of research will also be discussed.

2. Experimentally Observed SIPs

Currently, SIPs have mostly been observed in films of OSC molecules. There are several reasons for this: firstly, for the investigation of the suitability and properties of molecules to be used in organic electronic devices (e.g., organic field-effect transistors (OFETs), solar cells, etc.) molecules must be deposited onto a solid substrate; for a complete understanding of their behavior the structure that the molecules adopt in films must be determined, and therefore SIPs will be observed if they form. Secondly, one of most commonly used OSCs, pentacene, displays an SIP which must often be taken into account when performing studies using pentacene. OSCs also provide ideal systems for studying SIPs due to some of their common properties, such as lack of a strong dipole, simplicity of intermolecular interactions (often only van der Waals interactions), simple molecular shape (often elongated, rod-like molecules) and low conformational freedom (often fairly rigid). That is not to say that SIPs do not present themselves for other classes of molecules, e.g., pharmaceutical molecules where they could have a significant impact on properties, and their possible origins are discussed later in this article.

2.1. Pentacene

The best-known experimentally observed example of an SIP, and also the most-studied, is the thin-film phase of pentacene. Pentacene (**1**) (**Figure 2**), a member of the acene family of aromatic hydrocarbons, is an insoluble, ambipolar OSC which has long been an attractive material for use in OFETs due its relatively high charge transport mobility (>1 $cm^2 V^{-1} s^{-1}$ in ambient conditions) and ability to readily form ordered films.[53,54] These properties, along with the simplistic structure of the molecule and its ready availability, have made pentacene a benchmark material for organic electronics and the most-studied OSC compound in literature; at the time of writing there are over 17 300 publications relating to "pentacene" and over 2600 relating to both "pentacene" and "transistor" (Web of Science, June 23, 2015).

Pentacene forms with different structures and morphologies depending on the growth conditions and, in the case of films, on the type of surface it is deposited on. When deposited on graphene or metals, such as Au or Cu, pentacene molecules generally lie flat on the substrate surface,[55–57] while edge-on configurations may also be observed under specific conditions.[58] In contrast, when deposited on polymer surfaces, self-assembled monolayers or amorphous silica (SiO_x),

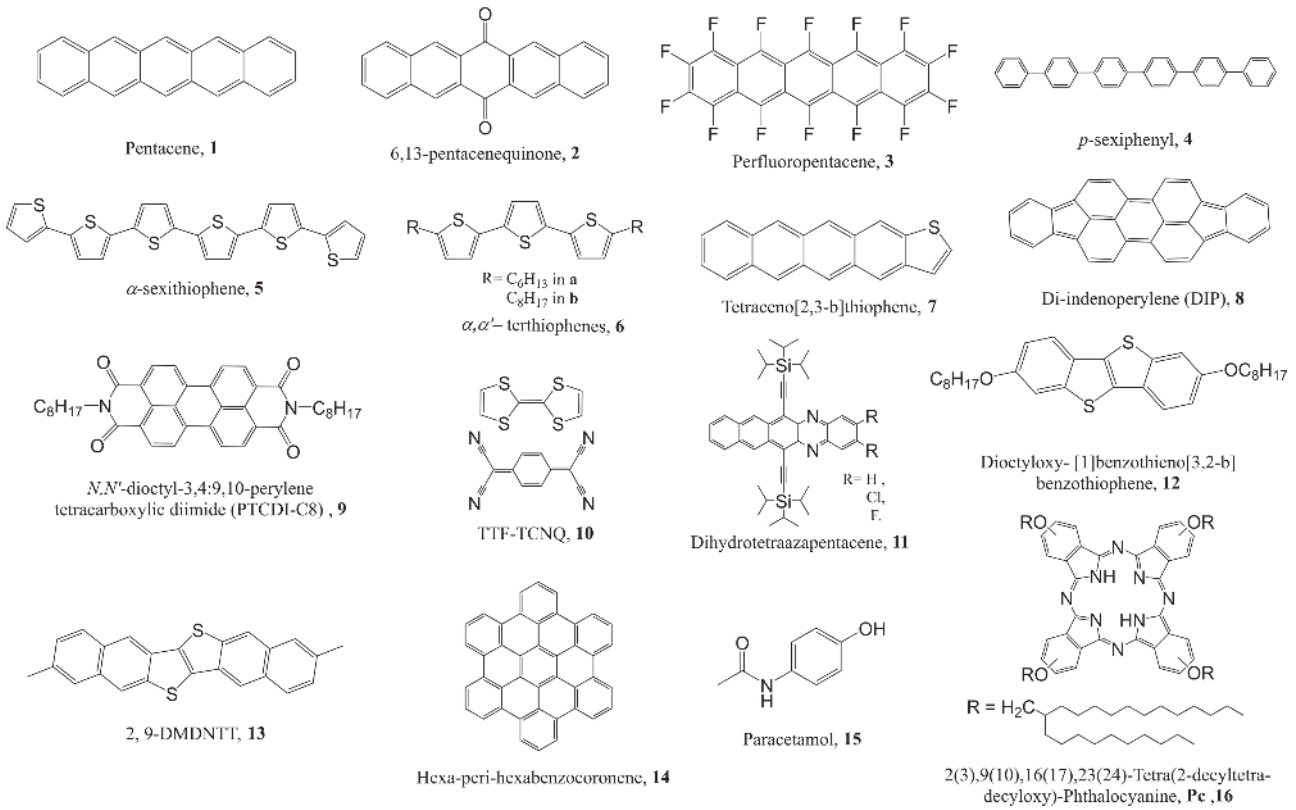

Figure 2. Examples of molecules for which substrate-induced phases (SIPs) have been observed in the vicinity of a solid substrate.

the molecules stand approximately upright, with a slight tilt of the long molecular axis away from the surface normal depending on which polymorph is present.[59–62] An alternative arrangement occurs in submonolayer and monolayer films, where molecules stand vertically on the substrate surface with no tilt away from the surface normal;[63,64] it should emphasized here that the monolayer structure of pentacene does not constitute a SIP as it does not extend over multiple molecular dimensions and the same is true for other monolayer structures. The difference between pentacene polymorphs can always be related to a change in the tilt of the long molecular axis, all polymorphs pack with layers of molecules in a herringbone arrangement and two molecules in a triclinic unit cell; polymorphs are normally identified by their characteristic (001) *d*-spacings corresponding to the out-of-plane lattice spacing in films on SiO_x substrates (**Table 1** and **Figure 3**).[59,65]

The two bulk structures of pentacene are the polymorphs which may both be observed in single crystal form. The first was characterized by Campbell et al. and has a characteristic (001) *d*-spacing of ≈14.4 Å;[67,71] this phase is known as either the Campbell phase or the high temperature (HT phase). A second bulk polymorph was characterized later with a characteristic (001) *d*-spacing of ≈14.1 Å; this phase is generally known as the low temperature (LT phase).[65,66,72] The LT phase is suggested to be unstable in films and the HT phase is therefore the bulk phase most commonly observed in thicker pentacene films,[73] while the LT phase is more commonly observed from single crystal growth of pentacene.[65] The LT phase is found to convert to the HT phase at elevated temperatures,[74] with the HT phase

Table 1. Unit cell parameters of the LT[66] and HT[67] bulk polymorphs, SIPs (SIP-1 corresponds to the 15.4 Å phase[68] found on SiO_x substrates, SIP-2 corresponds to the 15.1 Å phase[69] found on Kapton/NaCl substrates) and monolayer[63] structures of pentacene.

Phase	a [Å]	b [Å]	c [Å]	α [°]	β [°]	γ [°]	V [Å^3]	*d* (001) [Å]
LT (bulk)	6.28	7.71	14.42	76.75	88.01	84.52	677	14.1
HT (bulk)[a)]	6.06	7.90	15.01	81.6	77.2	85.8	692	14.4
SIP-1	5.92	7.54	15.63	81.5	87.2	89.9	689	15.4
SIP-2	6.1	7.6	15.3	81.0	85.0	89.5	698	15.1
Monolayer	5.916	7.588	–	–	–	84.7	720	16.1

[a)]A different choice of unit cell vectors from the original publication are used here.

Adv. Funct. Mater. **2016**,
DOI: 10.1002/adfm.201503169

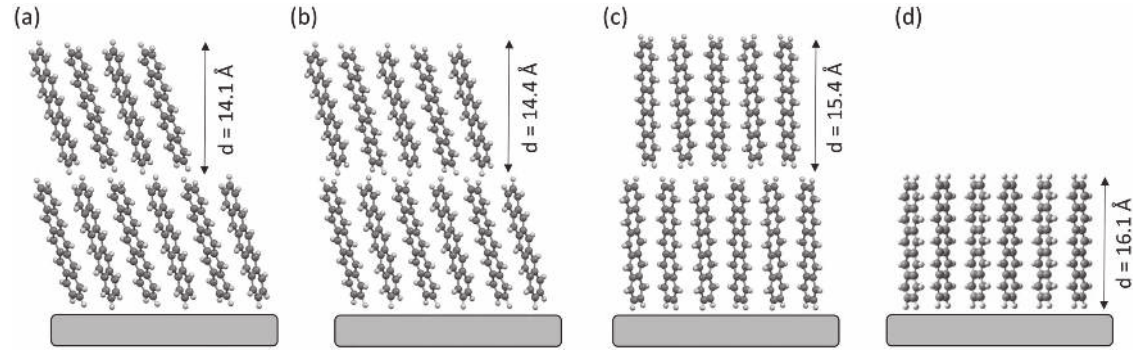

Figure 3. Different packing motifs of pentacene molecules observed in thin films where the precise molecular packing is known: a) molecules in the bulk (LT) phase with a tilt of ≈24° from the substrate normal,[66] b) molecules in the bulk (HT) phase with a tilt of ≈21°,[67] c) molecules in the common 15.4 Å SIP with a less pronounced tilt of ≈3°[70] and d) upright-standing molecules (0° tilt) in a monolayer.[63,64]

converting to the LT phase at high pressure.[75] The structural difference between these two bulk polymorphs arises from a shift of adjacent herringbone packed layers with only very slight differences observed in the packing within each layer.[74]

In films of pentacene on SiO_x substrates, larger (001) *d*-spacings were first observed by Minakata et al.,[76,77] however it was Dimitrakopoulos et al. who attributed these diffraction peaks to a new metastable, "thin-film" polymorph or SIP with a characteristic (001) *d*-spacing of 15.4 Å.[42] The HT bulk phase and SIP of pentacene were found to coexist in the same film above a certain critical film thickness (≈50 nm), with two different peaks clearly visible in specular X-ray diffraction scans (**Figure 4**). The observation that charge transport capabilities were hindered in mixed phase films compared with thinner films where only the SIP was present showed the potential impact of the presence of the SIP.[42,78] When solved by a combination of first-principles calculations and grazing incidence X-ray diffraction (GIXD) (Figure 4), the crystal structure of the SIP showed a reduced tilt of the long molecular axis compared with the bulk polymorphs and an interlayer packing closer to the HT phase than the LT phase (Figure 3b).[68,70,79] Crucially, the 15.4 Å SIP is found to be relatively unstable, converting to the HT bulk phase at elevated temperatures and with film aging;[80–82] various methods have been employed to attempt to understand and control the phase formation by solvent[83–85] and postannealing,[80,86] controlling film thickness,[87–89] limiting the conversion of the SIP to the bulk phase using capping layers[80] or deposition of films on rough surfaces to preferentially form the bulk phase.[90]

A second SIP of pentacene, with a (001) *d*-spacing of 15.1 Å, has also been observed to form on certain surfaces such as Kapton and NaCl.[59,69] In thicker films, the LT bulk phase, as opposed to the HT bulk phase observed in thick films containing the 15.4 Å SIP, is observed producing mixed phase films.[59] The 15.1 Å SIP is also found to be relatively unstable, converting to the LT phase at elevated temperatures,[59] while, interestingly, a transformation from the 15.4 Å SIP to the 15.1 Å SIP also occurs within pentacene OFETs after long term usage[91] and a similar effect is observed from the HT to the LT phase after device usage[92] which has also been shown to induce a strain in the film structure.[93] The mixing of the HT bulk phase and 15.4 Å SIP and mixing of the LT bulk phase and 15.1 Å SIP suggests an improved compatibility between their respective interlayer structures, allowing one to grow on

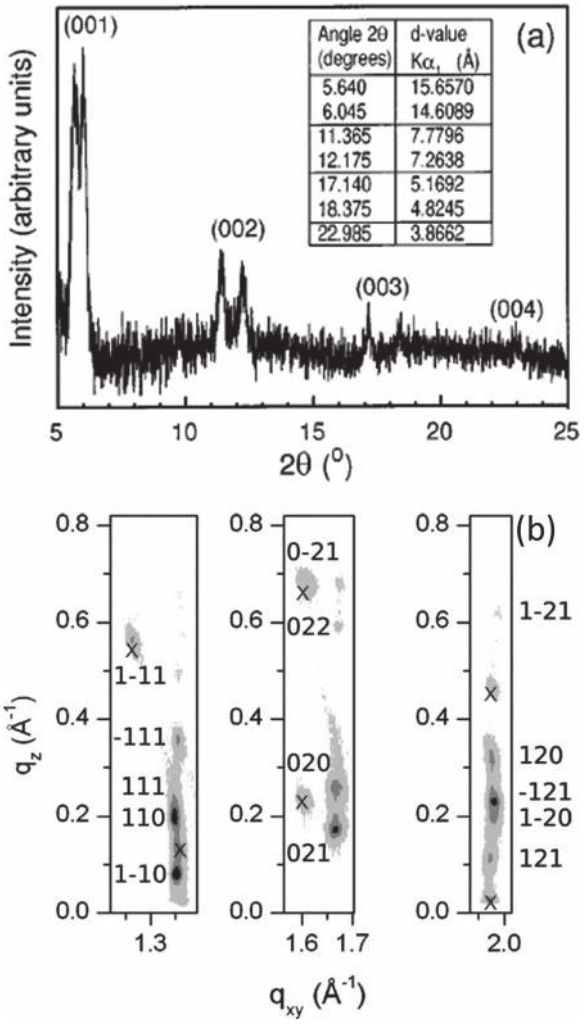

Figure 4. a) Specular X-ray diffraction pattern of thick and thin pentacene films showing the (001) and higher order reflections of the HT bulk phase (14.60 Å) and SIP (15.66 Å) Reproduced with permission.[42] Copyright 1996, American Institute of Physics. b) Indexed reciprocal space map generated from grazing incidence X-ray diffraction (GIXD) data with peaks from the HT bulk phase indicated by crosses and peaks corresponding to the SIP marked by their Miller indices. Reproduced with permission.[68] Copyright 2007, American Physical Society.

the other, with this being the most significant difference in the packing between the HT and LT bulk phases;[74] e.g., the 15.4 Å SIP has a similar interlayer packing motif to the HT bulk phase with which it can coexist with in thicker films (Figure 3).[79] It has also been suggested that the LT phase is destabilized in films compared to the HT phase due to the presence of the substrate and free surface effects, however this did not take account of the layer history within the film below the bulk phase (i.e., the presence of the SIP).[73] With the majority of pentacene films being grown on SiO_x substrates, the 15.1 Å SIP is not observed as often as the 15.4 Å SIP and has therefore not undergone the same degree of study.

Recently, a potentially new SIP of pentacene was observed with a (001) *d*-spacing of 13.5 Å in films coated onto polyimide nanogratings.[94] Tuning of the nanograting width could be used to control the proportion of the bulk phase present, but a high curvature of the nanograting surface was found to induce the new 13.5 Å polymorph. This form was also shown to be more stable than the bulk and SIP forms, with conversion from both to the 13.5 Å phase over time. While this is the only recorded example of the 13.5 Å polymorph, this finding highlights the possible role played by substrate geometry in determining the resulting the crystal structure, just as growth on a flat surface induces the more commonly observed 15.4 Å SIP of pentacene.

Another example of a member of the acene family displaying an SIP is found in films of tetracene which consists of four fused rings as opposed to the five in pentacene. Two different SIPs have been observed to form which could also be identified by X-ray diffraction from an increase in the out of plane (001) *d*-spacings;[95,96] this again suggests a decrease in the tilt of the upright-standing molecules with respect to the substrate, similar to what is observed in films of pentacene. High deposition rates are found to favor the SIP with the smallest molecular tilt from the surface normal and the two SIPs, which are found to coexist within films, have been observed on both SiO_x and Mylar substrates. Acenes such as pentacene, where the polymorphic behavior has been studied in detail, provide a good a basis for the understanding of the origins of SIPs.

2.2. Other Examples from Molecular Crystals

Two pentacene derivatives, 6,13-pentacenequinone (**2**) and perfluoropentacene (**3**), also exhibit SIPs (Figure 2). The bulk single crystal structures of **2** and **3** are characterized by monoclinic unit cells with dimensions of $a = 4.951$ Å, $b = 17.784$ Å, $c = 8.170$ Å and $\gamma = 93.26°$ for **2**,[97] and $a = 15.51$ Å, $b = 4.49$ Å, $c = 11.45$ Å, and $\beta = 91.6°$ for **3**.[98] In thin films, **2** crystallizes in a triclinic crystal system (space group *P*-1) with unit cell parameters $a = 4.69$ Å, $b = 5.99$ Å, $c = 13.45$ Å, $\alpha = 77.8°$, $\beta = 84.1°$, and $\gamma = 81.1°$, indicating the formation of an SIP (**Table 2**);[99] the unit cell volume of 364.2 Å^3, with one molecule per unit cell ($Z = 1$), is almost half the volume of the single crystal phase (718.2 Å^3). However in both the bulk and the SIP, the number of molecules in the asymmetric unit remains the same ($Z' = 0.5$). In contrast to the single crystal phase of **2**, which exhibits a herringbone arrangement, the crystal packing corresponding to the SIP is characterized by a coplanar π–π stacking motif, showing the potential differences in packing between the bulk phase and SIP.[99]

Table 2. An overview of the differences in crystallographic structural properties between the bulk phase and SIPs (in italics) of the compounds discussed. *Z* is the number of formula units within the unit cell, while *Z'* is the number of molecules in the asymmetric unit.

Compound	Crystal system	Space group	Unit cell volume [Å^3]	*Z*/*Z'*
1	Triclinic	*P*-1	692	2, 1
	Triclinic	*P*-1	*689*	*2, 1*
2	Monoclinic	$P2_1/b$	718	2, 0.5
	Triclinic	*P*-1	*364*	*1, 0.5*
3	Monoclinic	$P2_1/c$	797	2, 0.5
	Monoclinic	$P2_1/c$	*816*	*2, 0.5*
	Triclinic[1]	*P*-1	*820*	*2, 1*
4	Monoclinic	$P2_1/a$	1159	2, 0.5
	Monoclinic	$P2_1/a$	*1202*	*2, 0.5*
5	Monoclinic	$P2_1/n$	2117	4, 1
	LC-phase	–	–	–
6a[2]	Monoclinic	$P2_1/n$	6719	12, 3
	Orthorhombic	–	*38740*	*64,-*
6b[2]	Monoclinic	$P21/c$	2640	4, 1
	Orthorhombic	–	*2767*	*4, -*
7	Orthorhombic	$P2_12_12_1$	1335	4, 1
	Triclinic	*P*-1	*707*	*2, 1*
8	Triclinic	*P*-1	1991	4, 2
	Monoclinic	$P2_1/a$	*1028*	*2, 0.5*
9	Triclinic	*P*-1	769	1, 0.5
	Triclinic	*P*-1	*849*	*1, 0.5*
10	Monoclinic	$P2_1/a$	840	2, 0.5
	Monoclinic	$P2_1/a$	*839*	*2, 0.5*
11a	Triclinic	*P*-1	1860	2, 1
	Monoclinic	$P2_1/n$	*8055*	*8, 2*
12	Triclinic	*P*-1	1324	2, 1
	Monoclinic	–	*1439*	*2, 0.5*
13	Monoclinic	$P2_1$	880	2, 1
	–	–	–	–
14	Monoclinic	$P2_1/a$	1126	4, 1
	–	–	–	–
15[3]	Monoclinic	$P2_1/a$	741.9	4, 1
	Orthorhombic	*Pbca*	1458	8, 1
	Orthorhombic	$Pca2_1$	*1502*	*8, 1*
16	LC-phase	–	–	–
	Tetragonal	–	*11406*	*4, 1*

[1]Thin film on graphene coated substrate, [2]room temperature bulk phase and SIP have been considered. The space group is not evident from the GIXD data which was used to index the SIP. [3]The two polymorphic forms of **15** observed at room temperature are shown.

The crystal system of the SIP of **3** on SiO_x was found to be monoclinic, with unit cell parameters $a = 15.76$ Å, $b = 4.51$ Å, $c = 11.48$ Å, and $\beta = 90.4°$; the most significant deviation from the single crystal structure is the 0.25 Å elongation of the crystallographic *a*-axis with a β angle almost equal to 90°.[100] The

DOI: 10.1002/adfm.201503169

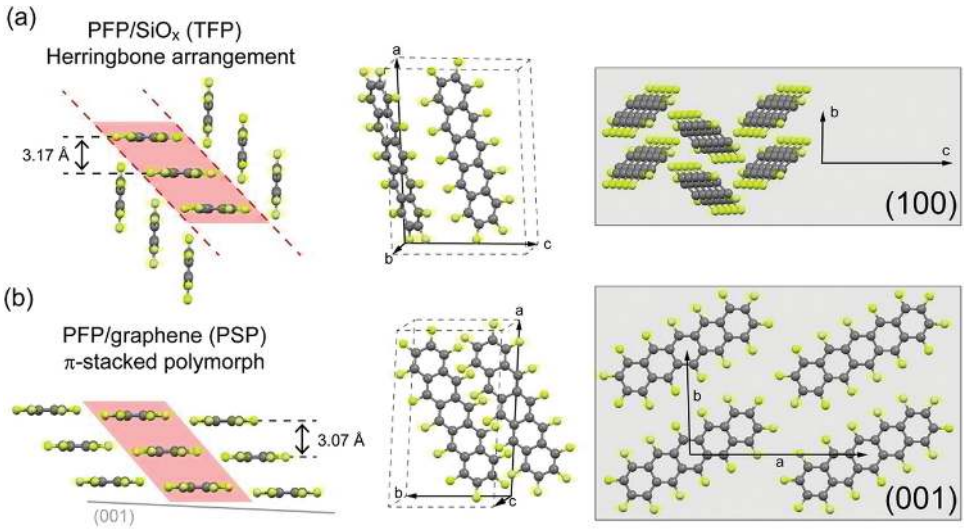

Figure 5. Comparison of the molecular arrangement in two SIPs of perfluoropentacene (**3**): a) Herringbone arrangement on SiO_x viewed along the long molecular axis (left), within the unit cell (middle), and as a top view of the (100) crystallographic plane (right). b) π-stacked arrangement of molecules on a graphene coated substrate viewed along the long molecular axis (left), within the unit cell (middle), and as a top view of the (001) crystallographic plane parallel to graphene (right). Similar π-stacked motifs in the two polymorphs are shaded in red with π-stacking distances also indicated. Adapted with permission.[102] Copyright 2012, American Chemical Society.

unit cell volume of the SIP (816.0 Å^3) is slightly larger than that of the single crystal structure (797 Å^3). The single crystal structure of **3** and the SIP both exhibit a herringbone packing arrangement with two molecules in the unit cell.[100,101] These changes from the bulk to the SIP of **3** are analogous to the differences in the structures of pentacene (**1**). For graphene coated substrates, a new SIP of **3** was found and it's structure was determined by a combination of GIXD and confocal Raman spectroscopy and found to have a triclinic unit cell with lattice parameters of a = 15.13 Å, b = 8.94 Å, c = 6.51 Å, α = 78.56°, β = 108.14° and γ = 92.44°, yielding a cell volume of 820 Å^3.[102] The crystal packing of the SIP on graphene is governed by coplanar π-stacked molecules. The π–π distance of 3.07 Å is significantly less than those observed in the herringbone packed structures of the bulk single crystal phase (3.26 Å) and the other SIP (3.17 Å) (**Figure 5**).

p-sexiphenyl (**4**) (Figure 2) is another OSC which consists of conjugated rings, but as each ring is only bonded to the next at one position it is more flexible than the pentacene derivatives (**2** and **3**) already discussed and the rings are able to twist relative to one another; this well-studied system has photoluminescent properties and potential applications in organic opto-electronic devices.[103,104] In single crystals, molecules are found to adopt a layered herringbone packing motif similar to pentacene with a monoclinic unit cell of dimensions a = 26.24 Å, b = 5.57 Å, c = 8.09 Å and β = 98.17° with V = 1159 Å^3,[105] while it was found that an SIP can form in thin films when deposited with a high substrate temperature.[106,107] The SIP is also found to be monoclinic with unit cell parameters a = 7.98 Å, b = 5.54 Å, c = 27.64 Å and β = 99.8° and an increased volume of 1202 Å^3. The difference between the SIP and bulk structures is similar to the examples of **1** and **3** on SiO_x, where the molecules maintain an upright-standing, herringbone packing motif in the SIP but with a reduced tilt of the long molecular axis with respect to the substrate normal.

A similar OSC molecule to **4** which also is known to form an SIP in films is α-sexithiophene (**5**), where the phenyl rings of **4** are replaced with thiophene rings (Figure 2). A low temperature single crystal structure was determined to consist of approximately planar molecules in herringbone packed layers,[109] similar to **4** and **1**; the structure of a high temperature polymorph has also been determined where the molecules show an increased tilt of the long molecular axis when compared to the low temperature bulk phase.[110] An SIP is found to form when grown as a film on SiO_x surfaces at high deposition rates, suggesting that the SIP formation is under kinetic control;[111–113] the SIP is suggested to be a disordered layered phase (order within layers but no correlation between layers) where the molecules have a reduced tilt compared with the low temperature bulk phase which also forms in films. In-situ GIXD experiments with different substrate temperatures reveal that growth of the SIP is favored at low substrate temperatures and is only prominent close to the substrate up to a certain critical thickness (≈8 nm) (**Figure 6**); above this thickness the growth of the bulk phase is dominant, though there is still some templating effect of the SIP leading to further SIP domains.[108] The monolayer structure has also been determined and it was shown that, as in previous examples, the molecules stand perfectly upright before tilting as growth of a multilayer film develops.[114] The example of α-sexithiophene (**5**) highlights the role that preparation parameters play in determining whether growth of the SIP or bulk phase is favored.

SIPs have also been observed for even more flexible molecules, this is perhaps unsurprising as flexible molecules have a strong tendency to form multiple polymorphs.[116] Two such systems where SIPs have been observed are for two dialkylated terthiophenes: α,α'-dihexyl-terthiophene (DHTT) (**6a**)[115] and α,α'-dioctyl-terthiophene (DOTT) (**6b**)[117] (Figure 2). In the case of **6a**, an SIP with a unit cell different to the two known bulk forms is observed by specular X-ray diffraction and GIXD

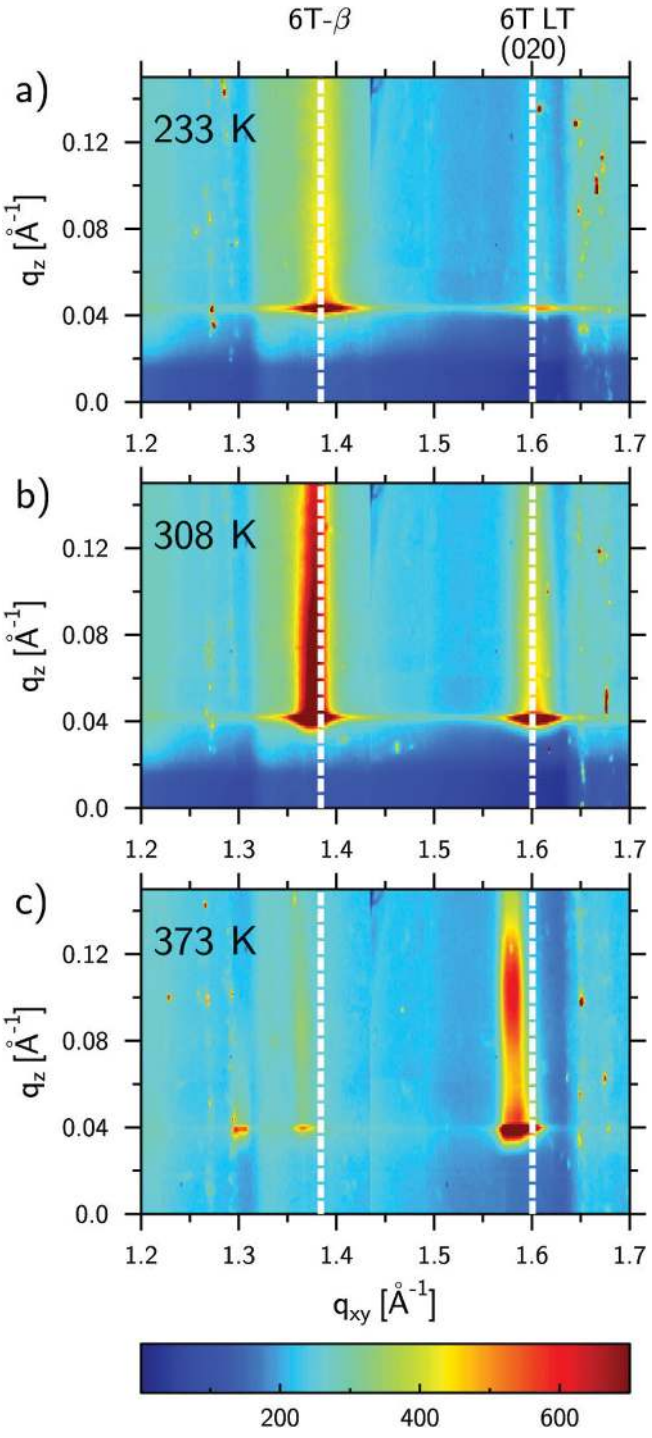

Figure 6. Reciprocal space maps generated from grazing incidence X-ray diffraction data of α-sexithiophene (**5**) films grown at a) 233, b) 308 and c) 373 K. White dashed lines indicate reflections arising from the SIP. Reproduced with permission.[108] Copyright 2015, American Chemical Society.

in solution cast (spin coated, drop cast and dip coated) films where crystallization is rapid (i.e., far from thermodynamic equilibrium), with the bulk form dominating when crystallization is allowed to proceed more slowly (**Figure 7**); the SIP is also observed in films produced by physical vapor deposition, a process which is also far from thermodynamic equilibrium.[115] A wetting layer containing flat-lying molecules was also found to be present at the substrate surface in samples where the SIP formed. It was shown that, for DHTT, the SIP is a metastable phase whose growth is determined by the crystallization kinetics and does not form when the system is closer to thermodynamic equilibrium.

For **6b**, a phase coexistence is observed where an SIP is found to form in the vicinity of the substrate while the bulk phase grows on top at the DOTT-air interface.[117] The relative amount of each phase present can be tuned by the changing substrate temperature during spin coating, with the SIP again favored at higher temperatures.[118] On heating to a LC or isotropic state, it was found that if the sample is cooled rapidly the SIP recrystallizes, while slow cooling favors recrystallization of the bulk phase.[117,118] These results serve to highlight an example where it is the thermodynamics of the system which govern which polymorph forms during deposition, while the metastable SIP can be trapped by rapid cooling from the LC phase or melt. The structure of the SIP was solved by a combination of GIXD and molecular dynamics simulations and was found to have terthiophene units packed side by side, while in the bulk forms they are shifted relative to one another (i.e., the molecules are interdigitated), showing that the structure of the SIP is adapted to conform to the planar substrate; the conformation of the alkyl side chains also differs depending on the polymorph.[119] The monolayer structure of **6b** was also investigated by X-ray reflectivity, (**Figure 8**) with the structure of the first monolayer still observed even as a multilayer films grow on top while a wetting layer was also observed beneath the monolayer.[119]

Tetraceno[2,3-*b*]thiophene (**7**) (Figure 2) is another pentacene analogue (with the terminal fused benzene ring replaced by a thiophene) which exhibits an SIP. The bulk crystal structure is characterized by an orthorhombic unit cell having parameters of $a = 5.92$ Å, $b = 7.64$ Å and $c = 29.52$ Å, with molecules adopting a herringbone crystal packing motif.[120,121] The structure of the SIP of **7** was found to be triclinic with a unit cell of $a = 5.96$ Å, $b = 7.71$ Å and $c = 15.16$ Å, $\alpha = 97.30°$, $\beta = 95.63°$, $\gamma = 90°$ and a unit cell volume of 707.6 Å^3,[122] almost half the volume of the single crystal phase (1335.2 Å^3); the herringbone motif observed in the single crystal phase is retained in the SIP. Interestingly, the antiparallel configuration of the molecules observed in the single crystal phase is no longer present in the SIP. When compared with **1**, the SIP of **7** has a similar in-plane geometry but a slightly different out-of-plane unit cell vector. The existence of the SIP was observed in films with a thickness of less than 20 nm and SIP formation was found to be independent of the substrate temperature and pre-deposition treatments.

The perylene derivatives, di-indenoperylene (DIP) (**8**) and *N,N′*-dioctyl-3,4:9,10-perylene tetracarboxylate diimide (PTCDI-C8) (**9**) (Figure 2) are two further compounds which display SIPs; **8** is a rigid molecule, while **9** has a rigid core with flexible alkyl side chains. Compound **8** shows an enantiotropic phase transition at 403 K from a low temperature triclinic phase (unit cell: $a = 11.659$ Å, $b = 13.010$ Å, $c = 14.966$ Å, $\alpha = 98.44°$, $\beta = 98.02°$, $\gamma = 114.54°$ and a volume of 1991 Å^3) to a higher symmetry monoclinic structure by an epitactic mechanism;[123] the low

DOI: 10.1002/adfm.201503169

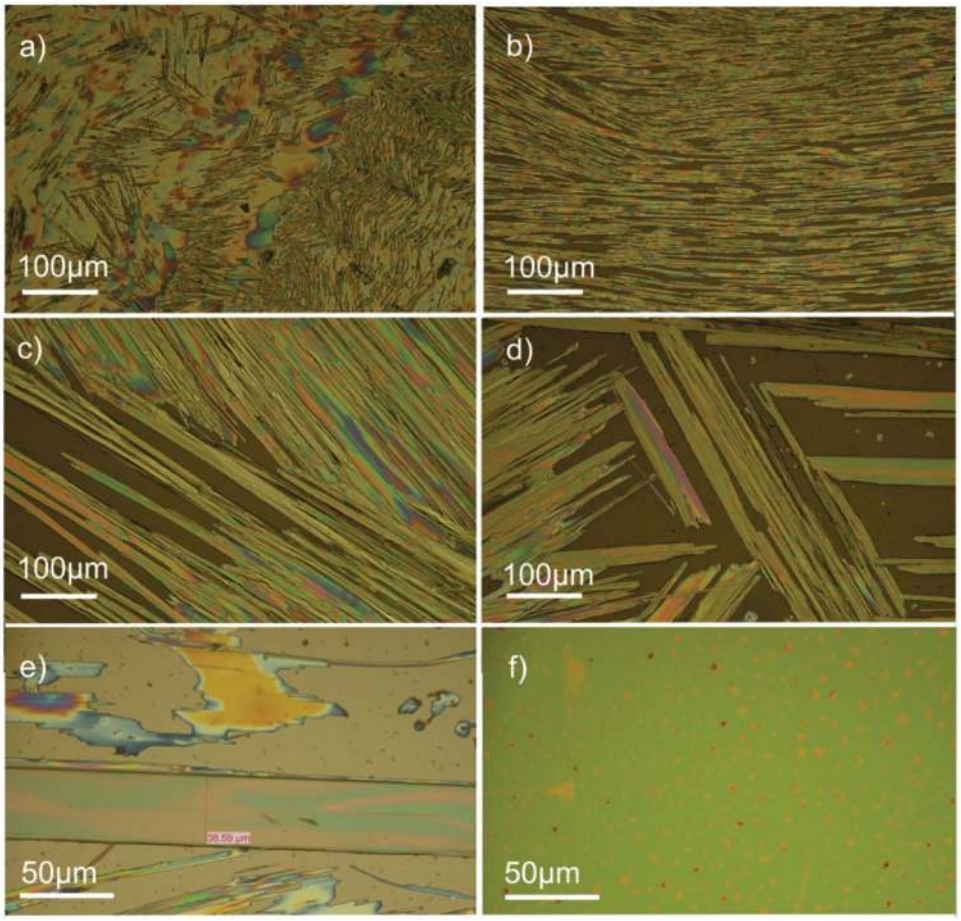

Figure 7. Optical microscopy images of DHTT (**6a**) films prepared by different methods. Drop cast films with solvent evaporation times of a) 2 min, b) 12 min, c) 75 min, d) 600 min and dip coated films with withdrawal speeds of e) 50 μm s^{-1} and f) 500 μm s^{-1}. The films shown in images (a) and (f) contain mostly the SIP while the remaining images show films containing mostly the bulk phase. Reproduced with permission.[115] Copyright 2012, Royal Society of Chemistry.

temperature phase contains two conformationally different molecules in the asymmetric unit. The high temperature monoclinic phase (β-phase) has lattice parameters of $a = 7.171$ Å, $b = 8.550$ Å, $c = 16.798$ Å, and $\beta = 92.416°$ and a unit cell volume of 1028 $Å^3$, with one molecule in the asymmetric unit. The transition can be understood in terms of a structural reorientation of the molecules involving bending and twisting distortions, loss of interdigitation due to a transformation of the two-dimensional herringbone layers to a more upright orientation, and finally, rearrangement of the layers by a shearing against each other (**Figure 9**). The SIP of **8**, as reported by Durr et al., is identical in structure to the high temperature β-phase.[124] It must be noted here that the substrate acts to stabilize the β-phase structure ≈200 K below the temperature where a phase transition to a low temperature phase is observed in the bulk.[125] In-situ GIXD measurements studying the film growth of **8** on different substrates showed that the first monolayer consisted of molecules in a more upright orientation, similar to the monolayer structure of **1**.[126] However, this structure was found to be transient and disappears on the addition of subsequent layers, with growth continuing in a strained layer-by-layer fashion until a rapid roughening occurs once the film is approximately 10 layers thick.

The thin film structure of **9** crystallizes in a triclinic unit cell with $a = 9.00$ Å, $b = 4.89$ Å, $c = 21.65$ Å, $\alpha = 95.0°$, $\beta = 100.7°$, and $\gamma = 112.8°$ with the crystallographic *ab*-plane parallel to the substrate (i.e., the (00*l*) planes are parallel to the substrate),[127] while the bulk single crystal structure has unit cell parameters of $a = 8.50$ Å, $b = 4.68$ Å, $c = 19.72$ Å, $\alpha = 88.43°$, $\beta = 94.01°$, and $\gamma = 97.21°$.[128] In bulk, the molecules of **9** exhibit a cofacial slipped π–π stacking along the crystallographic *a*-axis, with the nearest neighbor π–π distance being 3.24 Å. The SIP of **9**, in contrast, has the π-stacks along the crystallographic *b*-axis with a corresponding π–π distance of 3.58 Å. The tilt angle of the aromatic cores with respect to the substrate assumes a value of 67° in the SIP, in slight contrast to the 69.3° tilt angle observed in the bulk single crystal phase. The formation of an SIP has also been observed for the related molecule PTCDI-C5 when grown with substrate temperatures lower than 125 °C.[129] Interestingly, in another perylene derivative, PDI8-CN2, the same crystal structure is observed in thin films and in the bulk, i.e., no SIP is observed.[130] This was attributed to the high thermodynamic stability of the bulk phase preventing the formation of an SIP.

Tetrathiafulvalene–7,7,8,8-tetracyanoquinodimethane (TTF-TCNQ) (**10**) (Figure 2) is a well-studied charge-transfer (CT)

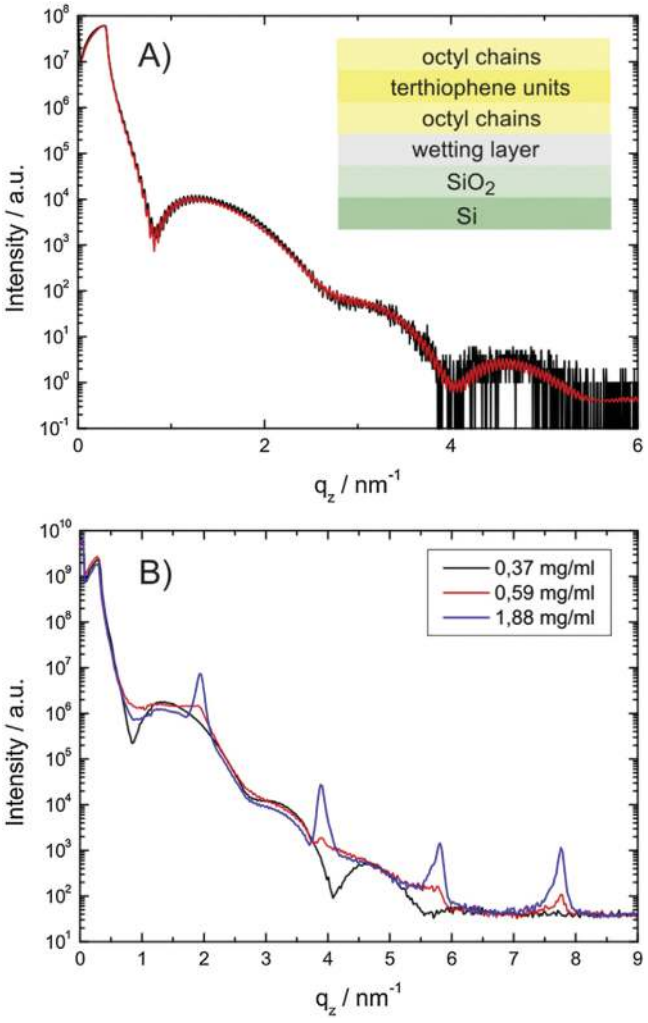

Figure 8. X-ray reflectivity curves of spin coated DOTT (**6b**) films. A) Experimental data (black) for a sample prepared from a 0.34 g L^{-1} toluene/tetrahydrofuran solution and the fitted curve (red) based on the model in the inset. B) Evolution of reflectivity curves and appearance of Bragg peaks as the solution concentration (correlated to the film thickness) is increased. Reproduced with permission under the terms of the CC-BY license agreement.[119] Copyright 2015, The Authors.

complex forming a quasi-one-dimensional conductor at room temperature. It has been recently reported that the crystal structure of thin films (monoclinic unit cell: a = 12.30 Å, b = 3.82 Å, c = 18.47 Å, β = 104.46°) deposited on KCl (100) is different when compared with the bulk structure (monoclinic unit cell: a = 12.26 Å, b = 3.77 Å, c = 18.69 Å, β = 103.76°).[131] Besides KCl (100), the SIP is also observed on SiO_x substrates, indicating that the formation of the thin film polymorph, i.e., the SIP, is not a consequence of epitaxy.[131] The crystal packing is essentially differentiated by a more upright molecular orientation in the SIP than in the bulk polymorph, similar to previous examples of SIPs (**Figure 10**). It is not clear exactly how the presence of an SIP impacts on the conducting properties of **10**, however changes in the preparation method and morphology are known to have an effect[132] and different properties have been suggested for different structures from theory,[133] so it is

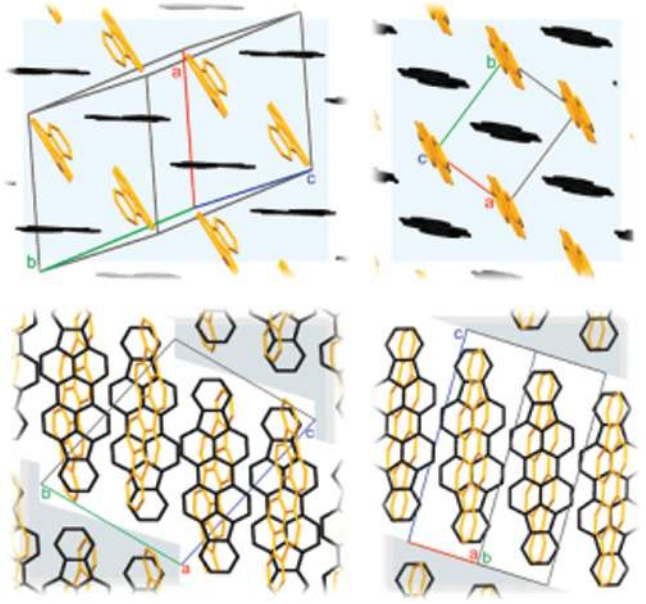

Figure 9. Herringbone layers of the low temperature (left) and the high temperature (right) phases of DIP (**8**). The twist and bend of molecules in the low temperature phase is shown. In the lower part, the herringbone packed layers are depicted from the side, showing the alignment of the rows of molecules. Reproduced with permission.[123] Copyright 2007, American Chemical Society.

likely that a change in the structure arising from an SIP would have a significant influence on the conducting properties of **10**. Polymorphism has been reported for several other CT complexes such as $(BEDT\text{-}TTF)_2I_3$ (BEDT-TTF = bis(ethylenedithio)-TTF)[134,135] and TMTSF-TCNQ (tetramethyltetraselenafulvalene-TCNQ);[136,137] in such complexes both the crystal structure and stoichiometry of the components are known to govern the physical properties.[138,139] Despite the known polymorphism in CT complexes, the presence of SIPs has not been explicitly mentioned in the literature and the example of **10** is, to the best of our knowledge, the only CT complex for which an SIP is known. As with other classes of molecules, SIPs may provide routes to CT complexes with properties different from those of the bulk forms and are therefore potentially very important.

Further examples of SIPs have been reported recently for a series of *N,N'*-dihydrotetraazapentacene (DHTA) derivatives which differ only in the substitution on the terminal ring (**11a–c** in Figure 2). Interestingly, in spin coated thin films of all three derivatives different polymorphic phases to those of the single crystals are observed.[140] The structure of the SIP of **11a** could only be resolved by growing a single crystal on the polyimide substrate and dissecting it for single crystal X-ray diffraction analysis. The one-dimensional column-like packing in the bulk phase of **11a** is transformed into a zig-zag molecular assembly when grown on the substrate, associated with a change in crystal system from triclinic (space group P-1) to monoclinic (space group $P2_1/n$). The results of specular X-ray diffraction experiments also reveal the presence of an SIP in **11b** on account of diffraction peaks which cannot be explained from the single crystal structure. For the thin films of **11c**, there appears to be a mixture of the bulk phase and other polymorphic

DOI: 10.1002/adfm.201503169

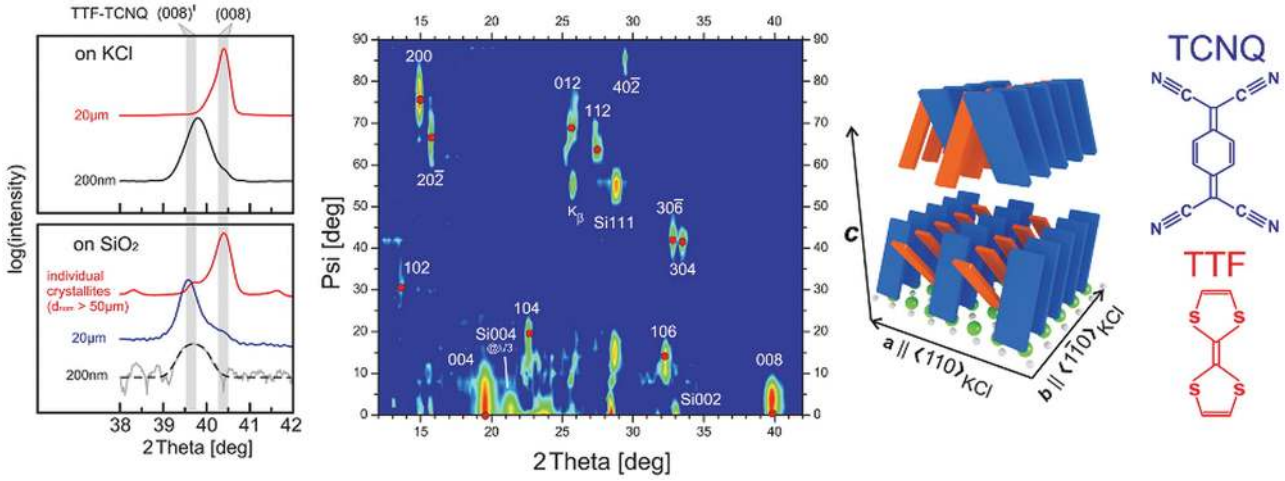

Figure 10. Specular X-ray diffraction patterns of TTF-TCNQ (**10**) films of differing thicknesses on KCl (001) and SiO_x, showing a magnified region around the (008) reflection (left). Reciprocal space map of the SIP of **10** obtained from films deposited on SiO_x (center). Simplified scheme showing the arrangement of molecules of **10** on a KCl (100) substrate (right). Reproduced with permission.[131] Copyright 2015, American Chemical Society.

forms. Although is a phase transition in **11c** around –73 °C, the structural modification is only a slight tilting of the brickwall motif observed in bulk single crystals. It is noteworthy that the specular diffraction patterns from films of all derivatives, **11a–c**, are similar, suggesting a common packing motif when crystallized on the substrate surface.

Another example of an SIP has been observed recently for a molecule in the [1]benzothieno[3,2-*b*]benzothiophene (BTBT) family of OSCs which have shown excellent charge carrier mobility properties.[141,142] An SIP was observed in films of the 2,7-dioctyloxy-BTBT (C_8O-BTBT-OC_8) derivative (**12**) (Figure 2),[143] unlike other dialkylated BTBT derivatives which have a layered herringbone packing in the bulk,[144] the bulk structure of **12** consists of π–π stacked, interdigitated molecules. In spin coated films of **12** studied by GIXD, molecules are found to adopt a herringbone packed structure similar to the bulk structure of other BTBT derivatives; this structure was found to be metastable, converting to the π–π stacked bulk structure over time and by solvent vapor annealing.[143]

Further interesting cases of SIPs are observed in systems related to dinaphtho[2,3-*b*:2′,3′-*f*]thieno[3,2-*b*]thiophene (DNTT): the 2,9- dimethyl substituted derivative (2,9-DMDNTT) (**13**)[145] and an isomer of DNTT, dinaphtho[1,2-*b*:2′,3′-*f*]thieno[3,2-b] thiophene (1,2-DNTT).[146] For **13**, a comparison of the X-ray diffraction patterns of thin films with those of a simulated bulk single crystal pattern revealed the presence of an entirely different structure in films. The interlayer spacing (*d*-spacing) is estimated to be ≈20 Å, indicating that **13** adopts a layered structure in thin films similar to the parent DNTT. This is in contrast to the bulk single crystal structure where a face-to-edge three-dimensional herringbone structure was found. Interestingly, in the isomeric 3,10-DMDNTT the structure observed in the bulk is preserved in thin films.[145] In films of 1,2-DNTT deposited at room temperature the molecules are found to adopt a more upright configuration when compared with the bulk single crystal structure or films deposited at 100 °C which also adopt the bulk structure. This was shown by X-ray diffraction measurements, with an increase in the out-of-plane *d*-spacing from 12.6 Å (in the bulk and films deposited at high temperatures) to 15.0 Å in films deposited at room temperature.[146]

A study on the thin film structure of hexa-peri-hexabenzocoronene (**14**) revealed that the crystal structure of films grown on graphene surfaces is different from that normally observed on SiO_x substrates.[147] The diffraction data coupled with a NEXAFS study revealed that the crystal packing changes from a herringbone motif to a coplanar π-stacked assembly. The observation of such a significant modification of the crystal structure in multilayer films on graphene compared to the bulk structure (planar arrangement vs. herringbone arrangement) has also been observed for perflouropentacene (**3**). Another recent study on contorted hexabenzocoronene revealed the presence of three different polymorphic structures in thin films which were accessible by post-deposition processing such as thermal annealing and solvent vapor annealing.[148]

There are several instances where a particular polymorph is stabilized by the substrate, similar to what has been observed for **8**, where the high temperature single crystal polymorph is similar to the SIP. For a further example we consider the case of paracetamol (**15**) (Figure 2), a very common and widely used pharmaceutical molecule. It is known that **15** has three different polymorphic forms: **I**, **II** and **III**. While form **I** has a monoclinic crystal structure, forms **II** and **III** crystallize with an orthorhombic structure. Form **III** is considered the least thermodynamically stable, with processes such as nanoconfinement being used to isolate it (**Figure 11**).[149–151] A study on thin films of **15** revealed that the metastable form **II** could be stabilized in dip coated films on a silica substrate,[152] while a further study showed that form **III**, the least stable form, can be stabilized on a silica surface by rapid heat treatment after deposition.[153] An SIP has also been reported for the pharmaceutical compound phenytoin which was found to have improved dissolution properties when compared with the bulk form;[154] such examples highlight the potential for a substrate to be used to stabilize metastable forms of drug molecules with enhanced properties.

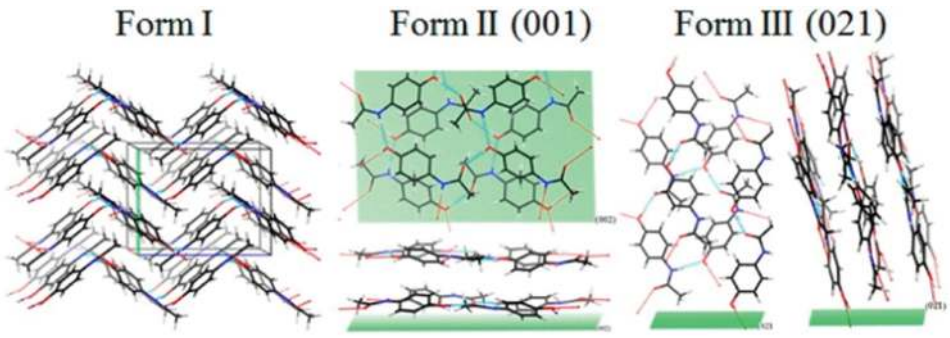

Polymorph	Form I	Form II	Form III
CSD code	HXACAN30	HXACAN08	HXACAN29
Temperature [K]	298	298	300
Space group	$P2_1/a$	Pbca	$Pca2_1$
a [Å]	7.01	17.17	11.84
b [Å]	9.21	11.78	8.56
c [Å]	11.60	7.21	14.82
β [°]	97.84	90.00	90.00

Figure 11. Visualization of the molecular arrangements within the crystal structures of paracetamol (**15**) forms **I**, **II**, and **III** together with the contact plane with respect to the SiO_x surface. The table summarizes the crystal lattice parameters with their corresponding Cambridge Structural Database (CSD) codes, space group, and the corresponding temperature at which the experiments were performed. Adapted with permission under the terms of the CC-BY license agreement.[153] Copyright 2014, American Chemical Society.

A similar example of a substrate stabilized polymorph has been observed for a 3,6-diaryl-2,5-dihydro-1,4-diketopyrrolo[3,4-*c*]pyrrole (DPP) derivative where one phase (α) is stable in the bulk, while the other phase (β) is more stable in thin films. The stabilization of the β-form in thin films is facilitated by solvent vapor annealing of films containing the α-phase. It is also possible for both polymorphic forms to be isolated in the bulk by varying the conditions during recrystallization.[155]

2.3. Examples from Liquid Crystals

LCs and plastic crystals (PCs) may qualify as ideal systems to study SIPs; in particular, they may allow simpler observation of a phenomenon which can be difficult to observe in crystalline systems.[156,157] Besides the example of the LC molecule 8CB discussed in the introduction, other molecular systems with considerably higher molecular weights and increased number of possible conformations also exhibit similar ordering behavior close to a solid substrate. The examples of alkylated hexa-peri-hexabenzocoronene[158] and of an alkoxy-substituted phthalocyanine derivative[159] show instances where changes in the interface properties allowed a specific molecular alignment to be achieved. In the context of SIPs, it is worth mentioning studies on interface nucleation where it was shown that control over growth kinetics and heterogeneous nucleation at the substrate can facilitate a homeotropic alignment of molecules.[160,161] Unlike SIPs, which correspond to a structural arrangement different from the bulk, these examples represent cases where the substrate can stabilize a particular molecular orientation in thin films.

The alkoxy-substituted phthalocyanine derivative, Pc,[159] (**16**) (Figure 2) exhibits an interesting and complex example of an SIP. The bulk thermotropic properties of **16** are well characterized, it exhibits a columnar rectangular phase (Col_r) at room temperature, transforming into a columnar hexagonal phase (Col_h) at ≈58 °C, before the onset of melting upon further heating at ≈182 °C.[159,162] The study of the SIP of **16** showed that the structure is a columnar tetragonal (Col_{tet}) PC phase exhibiting three-dimensional order, markedly different from the bulk LC form with a columnar rectangular (Col_r) structure.[163,164] The SIP forms independent of the thickness of the films and the nature of the substrate, but it is dependent on the time for which the films are aged (**Figure 12**). A polarized optical microscopy (POM) image of an as-prepared 74 nm thick film of **16** is shown in Figure 12a along with a film aged for 3 months (Figure 12b), where dendritic growth of a new phase can be clearly observed; the differences are also observed by AFM and specular X-ray diffraction (Figure 12c,d). This is a unique example where the two-dimensional LC phase converts to a three-dimensional PC phase due to nucleation caused by the solid substrate over time scales of a month or longer. In this case, the SIP is the most thermodynamically stable phase, whose appearance and

DOI: 10.1002/adfm.201503169

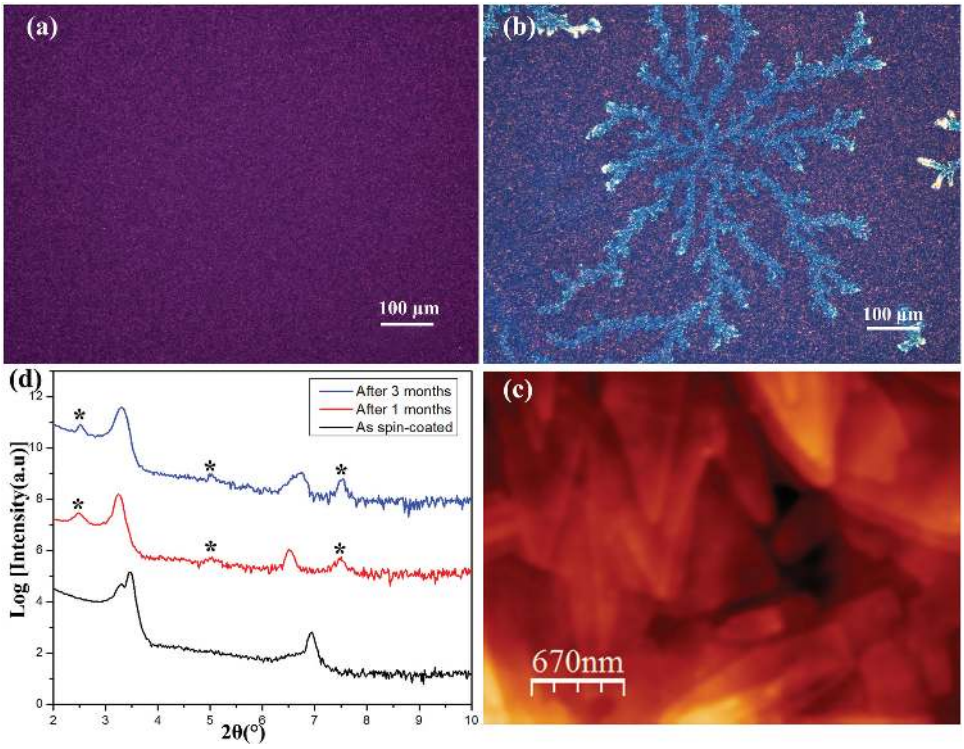

Figure 12. Polarized optical microscopy images of a 74 nm thick film of Pc (**16**) deposited on SiO_x substrates for an a) as-prepared spin coated film and b) a film aged for three months, showing the changes in film morphology. c) A tapping mode AFM phase image of the same film aged for 6 months. d) Specular X-ray diffraction patterns collected at various times for the same film; the plots are vertically shifted for clarity. The (100), (200) and (300) reflections from the SIP are marked with a star (*).

growth is a consequence of the geometrical effect imposed by the rigid and flat substrate, acting to catalyze the phase transition from, in this case, the less stable bulk LC phase to the PC phase. Also of interest is the fact that the SIP of **16** nucleating at the substrate is not restricted to the vicinity of the substrate but also grows on top of the bulk LC phase and a phase coexistence is present.

A similar structural transformation to a more ordered crystalline phase has also been observed in films of the LC perylene diimide derivative, *N,N′*-bis[3-[1,3-bis[2-(2-methoxyethoxy)-ethoxy]-2-propoxy]propyl]perylene-3,4,9,10-tetracarboxyldiimide (PPMEEM) (**Figure 13**). Spin coated films of PPMEEM were found to consist of randomly oriented polycrystalline domains; however, POM images obtained 24 hours after film preparation revealed the appearance of a highly ordered structure with a ribbon like crystalline morphology growing into the more disordered phase.

2.4. Effects of Polymorphism on Physical Properties

As demonstrated by the examples in the previous section, instances of polymorphism within organic thin films are not uncommon and so it is vital to understand the effect that changes in the solid state structure could have on the material properties.[166,167] As most of the examples reported here are OSC molecules, it is particularly relevant to understand the possible changes in electronic properties and device performance which could arise from a polymorphic system. While on the one hand polymorphism provides an excellent opportunity to establish structure-property correlations for different systems, on the other it presents a serious challenge for the fabrication, performance and reproducibility of devices such as OFETs.[168,169]

For a well-studied system like pentacene, there have been several studies which have shown the impact of polymorphism

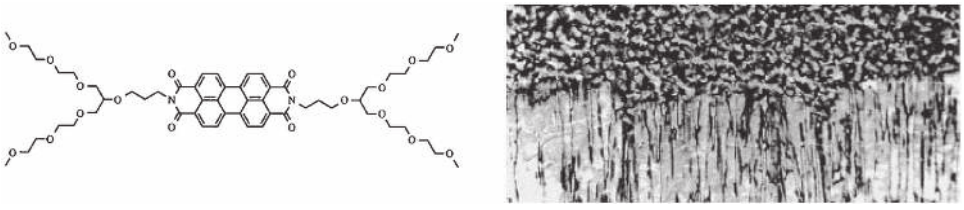

Figure 13. Chemical structure of PPMEEM (left) and a polarized optical microscopy (POM) image of a PPMEEM film (right). The lower portion of the POM image shows a highly crystalline region spontaneously growing into the less ordered region initially formed upon spin coating. Reproduced with permission.[165] Copyright 1997, American Chemical Society.

on device properties. One of the first studies on the structure of films of **1** by Dimitrakopoulos et al.[42] showed that OFETs consisting purely of the 15.4 Å SIP had superior charge carrier mobility properties when compared with amorphous or mixed phase films consisting of the SIP and HT bulk phase, a finding also confirmed in another study.[170] A theoretical study by Troisi et al.[171] calculated and compared the band structures of four different polymorphs of **1** (the HT and LT bulk phases and the 15.1 and 15.4 Å SIPs). They showed that the band structure differs greatly for each polymorph and that the mobility tensor is highly anisotropic in three of the four polymorphs. The exception is the 15.4 Å SIP, which they suggest would be the optimal polymorph to use for the production of OFETs due to the difficulty in aligning the crystals for maximum charge transport efficiency in OFETs produced from the other polymorphs.

Another example where an SIP is present and the impact of changes in the molecular packing are evident is the example of 2,9-DMDNTT (**13**).[145] An isomer of **13**, 3,10-DMDNTT, has the same structure in the bulk as in thin films (a three-dimensional herringbone packed motif), while **13** forms an SIP with a layered packing motif in thin films and has a three-dimensional herringbone packed motif, slightly different to that of 3,10-DMDNTT, in the bulk. As both molecules are isomeric their electronic properties are very alike, with similar HOMO energy levels and HOMO-LUMO gaps; however, the charge carrier mobilities observed in OFETs of the two isomers are markedly different, with values of ≈0.8 $cm^2 V^{-1} s^{-1}$ for the herringbone packed 3,10-DMDNTT and only ≈0.4 $cm^2 V^{-1} s^{-1}$ for the layered SIP of 2,9-DMDNTT. This is in contrast to films of the related 1,2-DNTT where an SIP forms in films deposited at room temperature but little difference is observed in the transistor characteristics of films containing the different phases (bulk and SIP).[146]

Besides pentacene (**1**), 5,6,11,12-tetraphenyltetracene (rubrene) is perhaps the most extensively studied OSC molecule due to its high charge carrier mobilities. It must be stressed here that rubrene doesn't exhibit an SIP, but it has been shown to have several different polymorphs and is an excellent example of the importance of crystal structure to device properties. Four different polymorphs of rubrene are found in the literature, a monoclinic phase,[172] a triclinic form[173] and two orthorhombic polymorphs. The first orthorhombic form, with space group *Aba*2, was found for crystals grown from vapor in a vacuum using sealed ampoules.[174] The second orthorhombic phase,[175,176] grown by physical vapor transport and crystallizing in the space group *Cmca*, is the form which is extensively investigated for device properties; single crystal transistors of this polymorph exhibit a charge carrier mobility of up to ≈40 $cm^2 V^{-1} s^{-1}$.[177,178] The high values of mobility are attributed to the crystal packing which has a herringbone motif with a high overlap of the π-conjugated tetracene backbone.[179] In the monoclinic and triclinic polymorphs, device performance is significantly reduced due to the absence of π-stacking interactions in the monoclinic polymorph and the significant slippage of tetracene backbones relative to one another in the triclinic polymorph.[180] A comparative study on single crystals of the *Cmca* orthorhombic form and the triclinic form, both grown from solution, revealed that the orthorhombic form exhibited hole mobilities of up to 1.6 $cm^2 V^{-1} s^{-1}$, while the triclinic form showed lower charge carrier mobilities of only 0.1 $cm^2 V^{-1} s^{-1}$. [181,182]

A further example of a polymorphic OSC molecule is that of 6,13-bis(triisopropylsilylethynyl)pentacene (TIPs-pentacene), one of the most-studied solution-processable OSCs and known to exhibit polymorphism at high temperatures.[183] While it does not exhibit any SIPs in thin films, it has been shown that changes to the film structure, brought about by introducing lattice strain through a solution shearing process during deposition, could increase the hole mobility in devices from 0.4 $cm^2 V^{-1} s^{-1}$ (in unstrained films) to 4.6 $cm^2 V^{-1} s^{-1}$ (in strained films).[184] It was then found that a degree of control could be exercised over the formation of the strained, metastable forms by tuning the parameters during shearing (e.g., the solvent used and the solution concentration).[185] Further fine tuning of the solution shearing process allowed average hole mobilities of 8.1 $cm^2 V^{-1} s^{-1}$ to be obtained for the strained, non-equilibrium phase.[186] A further study, utilizing nanoconfinement effects to stabilize metastable phases of TIPs-pentacene, produced a new metastable polymorph and compared the electronic properties of the different equilibrium and non-equilibrium forms.[187] It was found that, despite having only small variations in the molecular packing, the electronic properties of the different polymorphs were significantly different, with several orders of magnitude difference found in the hole mobilities, highlighting the effect small changes in the molecular packing can have.

5,11-Bis(triethylsilylethynyl)anthradithiophene (TES-ADT) and its fluorinated derivative, 2,8-difluoro-TES-ADT (diF-TES-ADT) present other examples of compounds for which the relationship between polymorphism and device properties are explicitly discussed in the literature. Depending on the solvent used TES-ADT crystallizes in two forms in thin films: the α-form crystallized from THF solution is similar to the bulk single crystal form, while the β-phase crystallized from toluene was not previously known and is possibly an SIP.[188] **Figure 14** gives a summary of the TES-ADT unit cell parameters and a corresponding summary of the device performance. Since the crystal packing of β-phase is still under investigation it is difficult to correlate device properties with structural features of the two forms, but as seen in **Figure 15**c there is a considerable difference in mobility between the two forms.[188]

Crystals of diF-TES-ADT grown from solution show evidence of a reversible phase transition at 294 K.[189] The two polymorphs are classified as the low temperature (LT) and high temperature (HT) phase, both crystallizing in a triclinic unit cell with space group *P*-1. The difference in the structures of the two polymorphs was found in how the layers of molecules stack relative to one another (Figure 15a). The charge carrier mobility was measured as a function of temperature for both single crystals and thin films, with an increase from ≈1.05 $cm^2 V^{-1} s^{-1}$ at 250 K to ≈1.8 $cm^2 V^{-1} s^{-1}$ at 330 K observed in single crystal transistors. The rate of the increase in mobility with temperature was found to change sharply at the phase transition temperature, showing the effect of the changes in the crystal packing (Figure 15b).[189] A further study of OFETs produced from diF-TES-ADT showed the importance of crystal alignment to device properties, where an increase in charge carrier mobility by ≈2 orders of magnitude could be achieved by tuning the preparation parameters to favor a specific crystalline alignment.[190]

For contorted hexabenzacoronene films, different polymorphic forms can be accessed depending on the post-deposition

DOI: 10.1002/adfm.201503169

a

	Bulk (α phase)[21]	Thin film α phase	Thin film β phase
a	0.69 nm	0.67 nm	1.85 nm
b	0.74 nm	0.72 nm	2.22 nm
c	1.66 nm	1.67 nm	1.67 nm
α	96°	—	—
β	92°	—	—
γ	106°	107°	90°
Z	1	1	9
$A_{(001)}$	0.49 nm^2	0.46 nm^2	4.11 nm^2
Fabrication conditions	Solution-grown single crystals	Thin films by SAC (0.2 wt% in THF)	Thin films by SAC (0.2 wt% in toluene or chloroform)

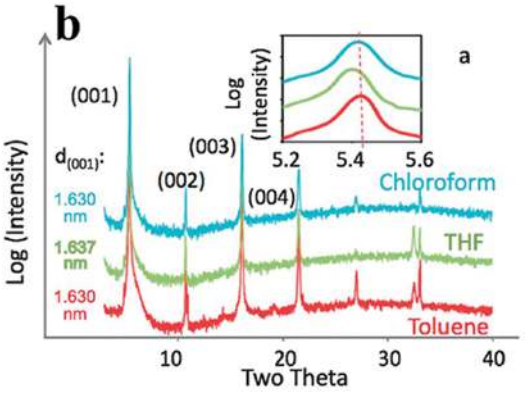

c

Solvent	Thin film polymorph	Mobility μ on PFBT/PTS (cm^2 V^{-1} s^{-1})	Mobility μ on PFBT (cm^2 V^{-1} s^{-1})
Toluene	β phase	0.22 ± 0.03	0.12 ± 0.07
THF	α phase	0.06 ± 0.01	9.7×10^{-3} ± 0.002

Figure 14. a) A summary of TES-ADT unit cells and preparation conditions. Thin films are grown by solvent-assisted crystallization (SAC); b) GIXD patterns of TES-ADT thin films slowly crystallized from chloroform, THF and toluene solutions. The films from chloroform and toluene share the same peak positions and hence the same structure; c) A summary of OFET device performance of TES-ADT thin films with pentafluorobenzenethiol (PFBT) treated electrodes and phenyltrichlorosilane (PTS) treated substrates (average values and standard deviations are obtained from 10 devices in each case). Adapted with permission.[188] Copyright 2014, The Royal Society of Chemistry.

processing of thin films (**Figure 16**a).[148] Different combinations of solvent vapor annealing (with THF) and thermal annealing could be used to access the previously unknown triclinic forms II and II'; form II' exhibits a similar diffraction pattern and structure to form II, but with slightly smaller lattice spacings (Figure 16b,c). A comparison of the charge carrier mobilities of devices constructed from films of forms II and II' with the same crystal orientation shows that devices containing pure form II' have an order of magnitude higher mobility than those of pure form II (Figure 16d,e). This again emphasizes the impact that small changes in the crystal structure can have on charge carrier mobilities, with an order of magnitude difference arising from only a slight shift of molecules.[148]

In a final example, it was recently shown that large changes in device performance could be observed in transistors made from a 9,9-diarylfluorine based OSC.[191] The as-deposited films have an amorphous structure, but exhibit an enantiotropic phase behavior and convert to a crystalline phase at ≈175 °C. Transistors containing the crystalline phase were found to have charge carrier mobilities approximately 2–3 orders of magnitude greater than those containing the amorphous phase. This behavior was in contrast to a related, monotropic 9,9-diarylfluroine derivate which showed little change in mobilities regardless of the temperature as only one phase exists in the films.

Taken together, the examples presented here show the impact that SIPs, and polymorphism in general, can have on physical properties relevant for organic thin film devices. While this list is not exhaustive, such examples highlight the importance of controlling the crystal structure in order to produce devices with properties tailored for their desired applications. While only OSC molecules have been discussed in this section, the same would hold true for other types of molecules, e.g., pharmaceutical compounds, where it would be desirable to tune other properties such as, for example, the solubility or environmental stability.

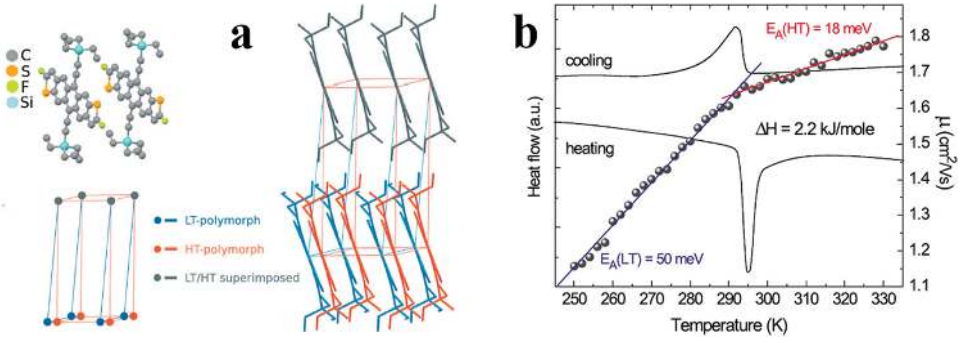

Figure 15. a) The crystal packing of the LT and HT polymorphs of diF-TES-ADT are shown. The first layers (top) of the two polymorphs are superimposed and shown in dark gray, the difference in the structures is clear in the second layer (bottom) where the molecules are shifted relative to one another; b) DSC curve of diF-TES-ADT; the evolution of the field-effect mobility (μ) with temperature for single crystal transistors is shown. The change in mobility around the transition temperature is clearly visible. Adapted with permission.[189] Copyright 2009, American Physical Society.

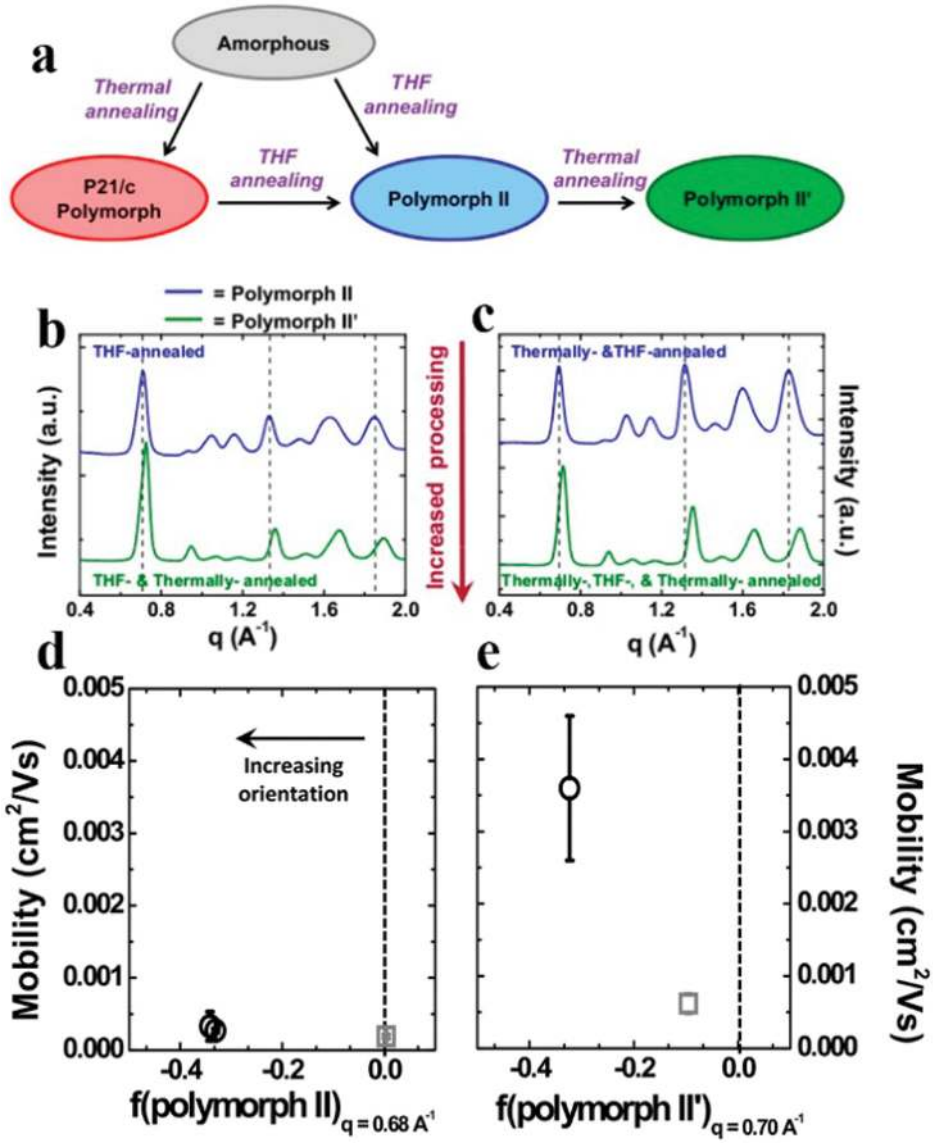

Figure 16. a) Schematic showing routes by which different polymorphs of contorted hexabenzacoronene can be obtained; diffraction patterns of thin films that were first either THF-annealed b) or thermally annealed and then THF-annealed, c) resulting in the films adopting polymorph II (blue curve). Subjecting each of these films to an additional thermal annealing step results in their transformation to polymorph II′ (green curve); mobilities plotted as a function of Herman's orientation function, *f*, for OFETs constructed from films containing d) polymorph II and e) polymorph II′. Reproduced with permission.[148] Copyright 2014, American Chemical Society.

3. Growth and Evolution of SIPs

To understand the formation of SIPs, it is necessary to study their nucleation and subsequent growth mechanisms in thin films. In this respect, it is useful to discuss the quintessential example of a polymorphic material, 5-methyl-2-[(2-nitrophenyl) amino]-3-thiophenecarbonitrile (commonly denoted ROY (red/orange/yellow) due to the colors of the different polymorphs).[192] ROY, with 10 known polymorphs, is an example where nucleation, growth and kinetic stability cannot be delinked and in fact play a concomitant role. According to the Ostwald rule of stages, the solute crystallizing out of a solution will crystallize first as the least thermodynamically stable polymorph, which then converts to the next least stable, and so on to the most stable form.[37] Although crystallization consists of both nucleation and growth, a common view is that the initial nucleation defines the final product polymorph(s);[193,194] however, this is not applicable in all cases. Studies of ROY have revealed a new mechanism of crystallization for polymorphic systems, cross-nucleation between polymorphs (where one polymorph acts as a seed for a different, faster-growing form which goes on to dominate the product crystal), which invalidates the view that the initial nucleation defines the final polymorph of crystallization.[192]

The formation of SIPs can be viewed as a similarly complex process. In fact, access to a particular structural form depends

DOI: 10.1002/adfm.201503169

on both thermodynamic and kinetic parameters, ultimately stemming from the subtle interplay between intra/inter-molecular, molecule–solvent (in the case of solution deposition) and molecule-substrate/interface interactions. On the other hand, it is reasonable to assume that homogeneous nucleation in solution rarely occurs experimentally due to the nearly unavoidable presence of dust particles which act as nucleation sites. The best evidence for this is that the ratio between the melting (T_m) and the crystallization temperatures (T_c) is commonly found to be $0.90 \le \frac{T_c}{T_m} \le 1.00$, whereas in ultrapure systems the value of $\frac{T_c}{T_m}$ goes down to ≈0.8,[195] even when slow cooling rates are used. However, if SIPs nucleate at the substrate surface then the experimental conditions leading to nucleation can, in principle, be much better controlled. The most controlled experimental conditions most likely occur for thin films grown from the vapor phase, with molecules landing on a clean substrate surface with known properties. As mentioned earlier, it has been found that organic thin film growth closely mimics the epitaxial growth of inorganic materials,[196] enabling an interpretation of organic thin film growth utilizing the concepts known from inorganic film growth.[197,198] Even in the absence of any epitaxial effects, growth modes of pentacene, tetracene, and perylene on substrates with which they have weak molecule-substrate interactions have been studied using the theory of nucleation for the epitaxial growth of inorganic materials.[199] The molecule-substrate interaction was found to be a crucial factor controlling the growth mode, i.e., a weaker molecule–substrate interaction tends towards three-dimensional growth, whereas stronger molecular interlayer interactions facilitates two-dimensional film growth.[199] The symmetric nature of inorganic systems enables a relatively straight-forward determination of the nucleation and growth modes from diffusivity, step energies and orientation independent interfacial energies; the inherent structural anisotropy of organic molecules creates a much more complex scenario where each molecule must overcome a reorientation barrier to align favorably on the substrate.[200] The relative molecular orientation thus governs the net free energy of the system. A schematic representation highlighting the different growth modes of inorganic and organic molecular systems is shown in **Figure 17**.

For certain organic systems the situation may be slightly less complex; for example, the growth modes of a spherical organic entity such as C_{60} are expected to be closer to those of an inorganic system. It is observed that C_{60} film growth follows an initial stage of two-dimensional island formation in a quasi-layer-by-layer manner on top of a C_{60} monolayer.[201] Moreover, the differences in surface topography on the nanoscale were found to predominantly determine the mode of film growth. A recent study aimed to provide an understanding of the growth dynamics of C_{60} films and showed that it exhibits both atom-like and colloid-like characteristics due to the short-ranged character of C_{60} interactions.[202]

For an understanding of the growth modes of an SIP, it is necessary to investigate its morphological signatures at different stages of growth. For pentacene (**1**) thin films it is observed that molecules diffuse on the substrate nucleating monolayer islands with fractal shapes;[200,203] these fractal shapes are characteristic features of diffusion limited aggregation.[204] This enabled an

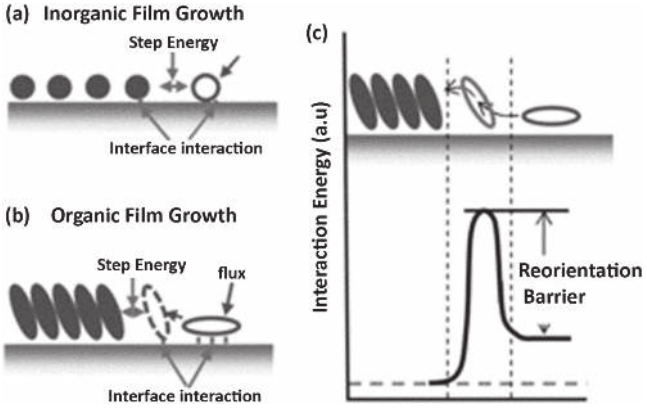

Figure 17. Schematic depicting the differences between nucleation and growth processes in inorganic and organic molecular systems: a) interfacial interactions for a diffusing atom are similar to those for an atom at a step edge; b) interfacial interactions for diffusing flat-lying molecules are different to those of a molecule at a step edge; c) the strength of interfacial interactions for a diffusing molecule determines the energy barrier for molecular reorientation. Reproduced with permission.[200] Copyright 2013, Wiley-VCH.

interpretation of the formation of the first layers of a film of **1** on SiO_x on the basis of diffusion-mediated growth.[205,206] However, theoretical studies have shown that there is a very small difference in the cohesive energy for the bulk phase (1.678 eV) and SIP (1.705 eV) of **1**.[207] Indeed, it has been shown that the bulk phase of **1** nucleates as early as the first monolayer, but growth of the SIP dominates during early film growth until a certain critical film thickness is reached, at which point growth of the bulk phase begins to dominate.[208] This shows that both phases coexist during film growth; once a bulk nucleus is formed it will continue to grow as a bulk phase crystallite with the SIP buried underneath leading to a saturation of the SIP thickness.

The transformation from the SIP to the bulk phase of **1** has been attributed to differences in surface energies of the two phases[87,209] as well as the surface stress.[89] This transformation is also evident as films of **1** are aged[82] or if they are exposed to solvent vapor.[83–85] A similar transformation is also observed for C_8O-BTBT-OC_8 (**12**) films if the sample is stored for a period of over 6 months or if it is subjected to solvent vapor annealing, which serves as a catalyst to accelerate the transformation to the bulk phase.[143] A transformation from the SIP to the bulk phase of **1** is also observed on heating above ≈400 K.[81]

The nucleation and growth of an SIP for a molecule like Pc (**16**) can be totally different.[164,210] In this case, the geometrical effect of the flat substrate acts as a stimuli to initiate nucleation of a crystalline phase, which is manifested as dendritic growth of the new phase on the surface and is present concomitantly with the bulk phase; aging of the films leads to formation of the SIP. The fractal shapes in this case too indicate growth by diffusion. Unlike **1**, here the SIP can be clearly distinguished from the bulk LC phase simply by optical microscopy. Only in films thinner than 10 nm is the bulk phase not observed due to limitations of the experimental techniques. Studies of molecular materials similar to **16** have not shown any formation of SIPs, indicating that it is an intrinsic material property and is dependent on the molecular structure.

4. Origins of SIPs

As discussed in the previous sections, a lot of research has been carried out to identify and characterize the presence of SIPs, but few explanations have been put forward to explain their origins. Although studies have suggested that the SIP of **1** converts to the bulk phase beyond a critical film thickness,[88] the exact mechanism involved in this transition is still unknown. The SIP of **1** can also be considered a strained metastable phase induced by the substrate where the transition from SIP to bulk phase is not continuous and both phases grow independently;[208] this is different to what is observed for heteroepitaxial growth where there is a steady transition to the bulk phase over several unit cell lengths as the film thickness increases.[211] Also, in the case of **16**, the SIP coexists with the bulk phase and, due to the limitations of experimental techniques, it is not clear if both phases are always present from the first layer onwards or if the bulk phase only appears above a critical film thickness. It is therefore difficult to come to any firm conclusions regarding the effect of film thickness while the mechanism of the transition from SIP to bulk phase is still unknown.

Some insights may be gained from theoretical studies on the SIP of **1**. Yoneya et al. used molecular dynamics simulations to attempt to understand the changes in the structural features of thin films of **1** going from the monolayer to thicker films.[212] The study revealed that the role of the substrate is negligible, in fact the structure of the SIP is dependent on the layer stacking history starting from the monolayer, i.e., the SIP containing tilted molecules forms due to the presence of the monolayer structure, consisting of upright-standing molecules, below. They also showed that the same monolayer structure would form even in the absence of substrate interactions.

For some systems, for example the OSC 2,7-dioctyl-BTBT (C8-BTBT), it is known that an interfacial or wetting layer, on top of which subsequent molecular layers grow, forms at the interface with the substrate.[213] The wetting layer, with a thickness of 0.6 nm, could be accounted for only if the molecules in this layer are considered to lie flat on the substrate, in contrast to the upright-standing configuration of the bulk film, though it is not clear if molecules are ordered within this layer. For films of **1**, it was also found that the nucleation density of the wetting layer in submonolayer films (≈1 nm nominal thickness) is very sensitive to the nature of the substrate.[214,215] Evidence of a wetting layer at the interface with the substrate was also found in films of **6a** where the SIP was present but not those where the bulk form was present,[115] while a wetting layer was also observed beneath the monolayer structure of **6b**.[119]

More generally, from studies of C_{60} it is revealed that different growth modes occur depending on if molecules are arriving on the substrate surface (in the case of the first monolayer) or on to a layer of C_{60} molecules (for layers after the first monolayer). C_{60} molecules can move easily on the substrate surface leading to the formation of thermodynamically favored round-shaped islands with a minimal boundary length, while for the growth of subsequent layers on C_{60} surfaces this process is kinetically hindered.[201] However, as C_{60} is a spherical system, it is not clear if the same would hold true for rod-like molecules, where a reorientation energy (from flat-lying to standing) may need to be accounted for. Following these examples, it may be logical to trace the origin of SIPs to the nature of the wetting layer or the monolayer underneath (i.e., the structure of the layer onto which deposited molecules arrive), whose structures are strongly dependent on the substrate. The importance of the monolayer structure to the formation of SIPs is highlighted by the examples of **1**,[64] **5**[114] and **6b**,[119] where the structure of the monolayer is different to that of the bulk phase and an SIP subsequently grows on top, whereas for a molecule such as C8-BTBT the monolayer structure is similar to the bulk structure and no SIP is observed[216] even though a strained metastable phase can form under specific preparation conditions.[142] Other systems present examples of wetting layers where lying molecules are present at the interface with the substrate but no SIP is observed, so the presence of an SIP may be due to the compatibility of the bulk structure with the structure of the wetting layer or monolayer below.[217] It is not clear if the relationship between a wetting layer and the layers above is epitaxial; it is often unclear if molecules are ordered within wetting layers and usually only an inference can made as to the molecular orientation within such a layer (e.g., flat-lying or upright-standing).

Some studies propose that the transition from the SIP to bulk phase is mainly driven by different growth conditions, rather than by the thickness of the film (i.e., by the distance from the substrate).[218] From the study of the SIP of **1**, it was expected that the critical thickness where the growth of the bulk phase begins to dominates over that of the SIP would be a function of the dielectric constant of the substrate.[87] In fact, thin film growth of **1** is highly sensitive to the precise nature of the surface[214,219] and it has been found that the substrate surface plays a crucial role in crystal nucleation and polymorph selection.[220] However, this does not appear to be universally applicable, as the SIP of **16** is observed on SiO_x substrates with a dielectric constant of $\varepsilon = 11.9$, and also on glass (SiO_2), poly-4-vinylphenol (PVP) and AlO_x substrates with dielectric constants of $\varepsilon = 3.9$, 5.0, and 9.9, respectively.[164,210]

A further growth condition which could influence SIP formation is the choice of deposition method. It might be expected that significant differences would be observed in the structure of films resulting from solution or vapor deposition techniques, as, for example, vapor deposition removes any contribution from solvent-molecule interactions. However, for **6a** the SIP forms in films produced by both physical vapor deposition and solution casting techniques (dip coating, spin coating and drop casting).[115] In fact it was found that the speed of crystallization was more important in determining the final phase, as slow dip coating and drop casting of films could produce films containing the bulk phase. Without further examples of systems where the behavior of films produced from vapor and solution deposition techniques has been studied in detail, it is difficult to definitively state the role played by the deposition technique in SIP formation, even if the growth mechanisms from vapor and solution processes are clearly different. However, it is known that the parameters chosen during film growth can have a significant effect on the film order, density and electronic properties.[221]

A substrate property which can play a role in SIP formation is the geometry of the substrate, which can be used to influence crystallization and hence the polymorphic form that

DOI: 10.1002/adfm.201503169

nucleates on the substrate.[222] For example, the rate of nucleation is found to be higher in grooves than on a flat surface and so crystallization first occurs in these locations.[222] A controlled substrate roughness, developed utilizing nanopores of different shapes, also shows that sharp angular shapes promote crystallization over spherically shaped nanopores.[223] In the context of SIPs, we can assume that the phase which matches best with the substrate geometry will be preferred. This has already been observed for **1**, where a new polymorph is formed when grown on polyimide nanogratings.[94] Such an effect can also be linked to the properties of the bulk structure, whereby a system with a bulk structure which has molecules protruding from unit cell faces (e.g., the examples of **6b** and **12**, where molecules are interdigitated in the bulk)[119,143] may be more likely to form an SIP when deposited on a flat substrate as the bulk structure does not conform to the substrate geometry when molecules adopt an upright-standing conformation.

Finally, the origin of SIPs can be traced to the nature of their crystal structures and differences from those of the bulk. Table 2 gives an overview of the properties of the crystal structures of the bulk phases as well as SIPs in order to highlight their structural differences. Although with a limited number of systems exhibiting SIPs it is difficult to systematically establish their nature, from Table 2 it is evident that in several cases there are no considerable changes in the crystal packing, with the only difference between the bulk phase and SIP corresponding to changes in the molecular tilt with respect to the substrate. However, going from the bulk to SIP there is a transition from a monoclinic to triclinic system for **2** and **3**, and from an orthorhombic to triclinic system in **7**; in films of **5** the bulk is monoclinic and the SIP is a disordered layered phase. Whereas for **8**, **11a** and **12**, the triclinic bulk phase converts to a monoclinic system. In **6a**, **6b** and **15** the transition is from monoclinic to orthorhombic and for **16**, the bulk LC-phase converts to a tetragonal PC phase. Thus, it appears that the systems with flexible side chains show a trend whereby there is a transformation to a more symmetric crystal structure in the vicinity of the substrate, while for rigid molecules the opposite may be true. However, a more substantial number of such examples would be required to justify such trends.

5. Outlook

In this article we have reviewed the current understanding of substrate-induced polymorphs and investigated materials which exhibit such behavior. A wide range of materials from rigid core aromatics, through pharmaceuticals, to flexible disordered liquid crystals have shown such structural characteristics. From the discussion on the growth characteristics and origins of SIPs, it is increasingly evident that they are an intrinsic material property. The inherent asymmetrical nature of organic materials is the crucial factor which controls their growth and the observation of such substrate-induced polymorphism can be attributed to this structural anisotropy. The origins of SIPs can be further traced to the structure of the wetting layer or monolayer which first forms at the interface with substrate. A systematic study of the crystal structures of SIPs reveals that molecules with flexible side chains are prone to convert to a more symmetrical crystal structure near the substrate surface, while there is some evidence that the opposite may be true for rigid molecules. It is also observed that the unit cell volume per molecule is generally larger in the SIP than in the bulk phase. For certain compounds like pentacene (**1**), C_8O-BTBT-OC_8 (**12**) or Pc (**16**), the SIP is transitory in nature, i.e., it transforms to the bulk structure either by aging or when initiated by an external stimulant such as temperature or solvent vapor. A better understanding of the phenomenon could likely be obtained by in situ studies; recent in-situ X-ray scattering studies show that they may be a powerful and useful tool to study SIPs.[224–226] Moreover, the growth mechanisms of the SIPs could also be monitored by in-situ imaging techniques.[227,228] Although SIPs are overwhelmingly observed for organic semiconductors, they are also important for pharmaceuticals, as shown by the example of paracetamol (**15**) and phenytoin. For any class of materials which has a tendency towards polymorphism, it may well be possible to observe SIPs and hence there is a necessity to characterize them. The fundamental outstanding questions which can be inferred from our study are: a) what are the exact growth mechanisms of SIPs and how is it linked with heterogeneous nucleation, b) does the molecular shape play a role, c) how does the chemical composition and nature of the substrate affect SIP formation and d) what are the thermodynamic and kinetic factors governing SIP formation. Obviously, future studies must be aimed at answering these questions. It would also be useful to have a repository of data (crystal and morphological) of SIPs along with the one which exists for the corresponding bulk structures (the Cambridge Structural Database). This would enable a systematic study of the changes a compound undergoes near the substrate surface. Finally, it is necessary for studies to be carried out to understand the formation of SIPs using theoretical modelling where it is possible to gain information inaccessible to current experimental techniques. Crystal structure prediction may be one such tool, although it can currently only be utilized to identify possible polymorphs and tally the results with the experimentally observed forms.[229] Understanding an SIP, however, involves modelling the role of the substrate (molecule-substrate interface as well as the molecule–molecule interface) and hence, the kinetics of crystallization. With SIPs of possible fundamental importance in many fields, and with the scope to form new polymorphs or stabilize metastable ones with potentially desirable properties, a deeper understanding of SIPs and their formation would bring significant advantages to many fields of research.

Acknowledgements

A.O.F.J. and B.C. contributed equally to this work. A.O.F.J. acknowledges financial support from the Austrian Science Fund (FWF): [P25887]. Financial support from FRS-FNRS (Belgian National Scientific Research Fund) for the POLYGRAD project (22333186), the Marie Curie IIF Scheme for the DISCO-project (project no. 298319 and 911319) and from the ARC program of the Communauté Française de Belgique (grant no. 20061) is kindly acknowledged by B.C and Y.H.G. B.C is a FRS-FNRS Research Fellow. Y.H.G. benefits from a Mandate of Francqui Research Professor from the Francqui Foundation.

Received: July 30, 2015
Revised: October 9, 2015
Published online:

[1] W. Drost-Hansen, *Ind. Eng. Chem.* **1969**, *61*, 10.
[2] W. D. Kaplan, Y. Kauffmann, *Annu. Rev. Mater. Res.* **2006**, *36*, 1.
[3] F. Ding, Z. Hu, Q. Zhong, K. Manfred, R. R. Gattass, M. R. Brindza, J. T. Fourkas, R. A. Walker, J. D. Weeks, *J. Phys. Chem. C* **2010**, *114*, 17651.
[4] P. G. Vekilov, *Cryst. Growth Des.* **2010**, *10*, 5007.
[5] G. A. Somorjai, Y. Li, *Introduction to Surface Chemistry and Catalysis*, John Wiley & Sons, New York/Chichester, UK **2010**.
[6] B. Bhushan, J. N. Israelachvili, U. Landman, *Nature* **1995**, *374*, 607.
[7] J. N. Israelachvili, D. Tabor, *Proc. R. Soc. Lond.* **1972**, *A331*, 19.
[8] J. N. Israelachvili, *Intermolecular and Surface Forces*, Academic Press, Waltham, MA, USA **1985**.
[9] C. S. Jayanthi, E. Tosatti, L. Pietronero, *Phys. Rev. B* **1985**, *31*, 3456.
[10] J. W. M. Frenken, P. M. J. Marée, J. F. van der Veen, *Phys. Rev. B* **1986**, *34*, 7506.
[11] J. G. Dash, *Contemp. Phys.* **1989**, *30*, 89.
[12] X. Wei, P. B. Miranda, Y. R. Shen, *Phys. Rev. Lett.* **2001**, *86*, 1554.
[13] X. Z. Wu, B. M. Ocko, E. B. Sirota, S. K. Sinha, M. Deutsch, B. H. Cao, M. W. Kim, *Science* **1993**, *261*, 1018.
[14] F. A. M. Leermakers, M. A. Cohen Stuart, *Phys. Rev. Lett.* **1996**, *76*, 82.
[15] B. M. Ocko, X. Z. Wu, E. B. Sirota, S. K. Sinha, O. Gang, M. Deutsch, *Phys. Rev. E* **1997**, *55*, 3164.
[16] B. M. Ocko, H. Hlaing, P. N. Jepsen, S. Kewalramani, A. Tkachenko, D. Pontoni, H. Reichert, M. Deutsch, *Phys. Rev. Lett.* **2011**, *106*, 137801.
[17] D. Demus, J. Goodby, G. W. Gray, H.-W. Spiess, V. Vill, *Handbook of Liquid Crystals*, Wiley-VCH, Weinheim, Germany **2008**.
[18] J. M. Geary, J. W. Goodby, A. R. Kmetz, J. S. Patel, *J. Appl. Phys.* **1987**, *62*, 4100.
[19] J. Stöhr, M. G. Samant, A. Cossy-Favre, J. Díaz, Y. Momoi, S. Odahara, T. Nagata, *Macromolecules* **1998**, *31*, 1942.
[20] B. W. Lee, N. A. Clark, *Science* **2001**, *291*, 2576.
[21] J. A. Castellano, *Mol. Cryst. Liq. Cryst.* **1983**, *94*, 33.
[22] T. Miyazaki, H. Hayashi, M. Yamashita, *Mol. Cryst. Liq. Cryst. Sci. Technol. Sect. Mol. Cryst. Liq. Cryst.* **1999**, *330*, 367.
[23] K. Kočevar, I. Muševič, *Phys. Rev. E* **2002**, *65*, 021703.
[24] L. Zhang, M. Kappl, G. K. Auernhammer, B. Ullrich, H.-J. Butt, D. Vollmer, in *Surf. Interfacial Forces – Fundam. Appl.* (Eds.: G. K. Auernhammer, H.-J. Butt, D. Vollmer), Springer, Berlin Heidelberg, Germany **2008**, pp. 39.
[25] J. Stöhr, M. G. Samant, J. Lüning, A. C. Callegari, P. Chaudhari, J. P. Doyle, J. A. Lacey, S. A. Lien, S. Purushothaman, J. L. Speidell, *Science* **2001**, *292*, 2299.
[26] J.-H. Kim, M. Yoneya, H. Yokoyama, *Nature* **2002**, *420*, 159.
[27] S. Kumar, J.-H. Kim, Y. Shi, *Phys. Rev. Lett.* **2005**, *94*, 077803.
[28] V. Coropceanu, J. Cornil, D. A. da Silva Filho, Y. Olivier, R. Silbey, J.-L. Brédas, *Chem. Rev.* **2007**, *107*, 926.
[29] S. Sergeyev, W. Pisula, Y. H. Geerts, *Chem. Soc. Rev.* **2007**, *36*, 1902.
[30] W. Pisula, M. Zorn, J. Y. Chang, K. Müllen, R. Zentel, *Macromol. Rapid Commun.* **2009**, *30*, 1179.
[31] F. Dinelli, M. Murgia, P. Levy, M. Cavallini, F. Biscarini, D. M. de Leeuw, *Phys. Rev. Lett.* **2004**, *92*, 116802.
[32] B. Rodŕıguez-Spong, C. P. Price, A. Jayasankar, A. J. Matzger, N. Rodŕıguez-Hornedo, *Adv. Drug Deliv. Rev.* **2004**, *56*, 241.
[33] B. A. Wacaser, K. A. Dick, J. Johansson, M. T. Borgström, K. Deppert, L. Samuelson, *Adv. Mater.* **2009**, *21*, 153.
[34] G. R. Desiraju, *J. Am. Chem. Soc.* **2013**, *135*, 9952.
[35] J. Bernstein, *Cryst. Growth Des.* **2011**, *11*, 632.
[36] J. Nyman, G. M. Day, *CrystEngComm* **2015**, *17*, 5154.
[37] W. Ostwald, *Z. Phys. Chem.* **1897**, *22*, 289.
[38] T. Threlfall, *Org. Process Res. Dev.* **2000**, *4*, 384.
[39] R. Hiremath, J. A. Basile, S. W. Varney, J. A. Swift, *J. Am. Chem. Soc.* **2005**, *127*, 18321.
[40] C. Capacci-Daniel, K. J. Gaskell, J. A. Swift, *Cryst. Growth Des.* **2010**, *10*, 952.
[41] L. H. Thomas, C. Wales, L. Zhao, C. C. Wilson, *Cryst. Growth Des.* **2011**, *11*, 1450.
[42] C. D. Dimitrakopoulos, A. R. Brown, A. Pomp, *J. Appl. Phys.* **1996**, *80*, 2501.
[43] F. Schreiber, *Prog. Surf. Sci.* **2000**, *65*, 151.
[44] D. E. Hooks, T. Fritz, M. D. Ward, *Adv. Mater.* **2001**, *13*, 227.
[45] A. C. Hillier, M. D. Ward, *Phys. Rev. B* **1996**, *54*, 14037.
[46] E. Umbach, K. Glöckler, M. Sokolowski, *Surf. Sci.* **1998**, *402–404*, 20.
[47] S. C. B. Mannsfeld, T. Fritz, *Mod. Phys. Lett. B* **2006**, *20*, 585.
[48] C. Wagner, R. Forker, T. Fritz, *J. Phys. Chem. Lett.* **2012**, *3*, 419.
[49] A. Koma, *Thin Solid Films* **1992**, *216*, 72.
[50] S. R. Forrest, Y. Zhang, *Phys. Rev. B* **1994**, *49*, 11297.
[51] T. Djuric, T. Ules, S. Gusenleitner, N. Kayunkid, H. Plank, G. Hlawacek, C. Teichert, M. Brinkmann, M. Ramsey, R. Resel, *Phys. Chem. Chem. Phys.* **2012**, *14*, 262.
[52] T. Djuric, T. Ules, H.-G. Flesch, H. Plank, Q. Shen, C. Teichert, R. Resel, M. G. Ramsey, *Cryst. Growth Des.* **2011**, *11*, 1015.
[53] S. Lee, B. Koo, J. Shin, E. Lee, H. Park, H. Kim, *Appl. Phys. Lett.* **2006**, *88*, 162109.
[54] M. Kitamura, Y. Arakawa, *J. Phys. Condens. Matter* **2008**, *20*, 184011.
[55] D. Käfer, L. Ruppel, G. Witte, *Phys. Rev. B* **2007**, *75*, 085309.
[56] N. Koch, A. Gerlach, S. Duhm, H. Glowatzki, G. Heimel, A. Vollmer, Y. Sakamoto, T. Suzuki, J. Zegenhagen, J. P. Rabe, F. Schreiber, *J. Am. Chem. Soc.* **2008**, *130*, 7300.
[57] W. H. Lee, J. Park, S. H. Sim, S. Lim, K. S. Kim, B. H. Hong, K. Cho, *J. Am. Chem. Soc.* **2011**, *133*, 4447.
[58] G. Bavdek, A. Cossaro, D. Cvetko, C. Africh, C. Blasetti, F. Esch, A. Morgante, L. Floreano, *Langmuir* **2008**, *24*, 767.
[59] C. C. Mattheus, A. B. Dros, J. Baas, G. T. Oostergetel, A. Meetsma, J. L. de Boer, T. T. M. Palstra, *Synth. Met.* **2003**, *138*, 475.
[60] B. Stadlober, U. Haas, H. Maresch, A. Haase, *Phys. Rev. B* **2006**, *74*, 165302.
[61] S. Nishikata, G. Sazaki, J. T. Sadowski, A. Al-Mahboob, T. Nishihara, Y. Fujikawa, S. Suto, T. Sakurai, K. Nakajima, *Phys. Rev. B* **2007**, *76*, 165424.
[62] H. S. Lee, D. H. Kim, J. H. Cho, M. Hwang, Y. Jang, K. Cho, *J. Am. Chem. Soc.* **2008**, *130*, 10556.
[63] S. E. Fritz, S. M. Martin, C. D. Frisbie, M. D. Ward, M. F. Toney, *J. Am. Chem. Soc.* **2004**, *126*, 4084.
[64] S. C. B. Mannsfeld, A. Virkar, C. Reese, M. F. Toney, Z. Bao, *Adv. Mater.* **2009**, *21*, 2294.
[65] C. C. Mattheus, A. B. Dros, J. Baas, A. Meetsma, J. L. de Boer, T. T. M. Palstra, *Acta Crystallogr. C* **2001**, *57*, 939.
[66] D. Holmes, S. Kumaraswamy, A. J. Matzger, K. P. C. Vollhardt, *Chem. Eur. J.* **1999**, *5*, 3399.
[67] R. B. Campbell, J. M. Robertson, J. Trotter, *Acta Crystallogr.* **1962**, *15*, 289.
[68] D. Nabok, P. Puschnig, C. Ambrosch-Draxl, O. Werzer, R. Resel, D.-M. Smilgies, *Phys. Rev. B* **2007**, *76*, 235322.
[69] J. S. Wu, J. C. H. Spence, *J. Appl. Crystallogr.* **2004**, *37*, 78.
[70] S. Schiefer, M. Huth, A. Dobrinevski, B. Nickel, *J. Am. Chem. Soc.* **2007**, *129*, 10316.
[71] R. B. Campbell, J. M. Robertson, J. Trotter, *Acta Crystallogr.* **1961**, *14*, 705.
[72] T. Siegrist, C. Kloc, J. H. Schön, B. Batlogg, R. C. Haddon, S. Berg, G. A. Thomas, *Angew. Chem. Int. Ed.* **2001**, *40*, 1732.
[73] M. Yoneya, M. Kawasaki, M. Ando, *J. Mater. Chem.* **2010**, *20*, 10397.

DOI: 10.1002/adfm.201503169

[74] T. Siegrist, C. Besnard, S. Haas, M. Schiltz, P. Pattison, D. Chernyshov, B. Batlogg, C. Kloc, *Adv. Mater.* **2007**, *19*, 2079.
[75] L. Farina, A. Brillante, R. G. Della Valle, E. Venuti, M. Amboage, K. Syassen, *Chem. Phys. Lett.* **2003**, *375*, 490.
[76] T. Minakata, I. Nagoya, M. Ozaki, *J. Appl. Phys.* **1991**, *69*, 7354.
[77] T. Minakata, H. Imai, M. Ozaki, K. Saco, *J. Appl. Phys.* **1992**, *72*, 5220.
[78] I. P. M. Bouchoms, W. A. Schoonveld, J. Vrijmoeth, T. M. Klapwijk, *Synth. Met.* **1999**, *104*, 175.
[79] H. Yoshida, K. Inaba, N. Sato, *Appl. Phys. Lett.* **2007**, *90*, 181930.
[80] T. Ji, S. Jung, V. K. Varadan, *Org. Electron.* **2008**, *9*, 895.
[81] A. Moser, J. Novák, H.-G. Flesch, T. Djuric, O. Werzer, A. Haase, R. Resel, *Appl. Phys. Lett.* **2011**, *99*, 221911.
[82] C. Westermeier, A. Cernescu, S. Amarie, C. Liewald, F. Keilmann, B. Nickel, *Nat. Commun.* **2014**, *5*, 4101.
[83] H.-L. Cheng, J.-W. Lin, *Cryst. Growth Des.* **2010**, *10*, 4501.
[84] A. Amassian, V. A. Pozdin, R. Li, D.-M. Smilgies, G. G. Malliaras, *J. Mater. Chem.* **2010**, *20*, 2623.
[85] D. J. Gundlach, T. N. Jackson, D. G. Schlom, S. F. Nelson, *Appl. Phys. Lett.* **1999**, *74*, 3302.
[86] S. J. Kang, M. Noh, D. S. Park, H. J. Kim, C. N. Whang, C.-H. Chang, *J. Appl. Phys.* **2004**, *95*, 2293.
[87] L. F. Drummy, D. C. Martin, *Adv. Mater.* **2005**, *17*, 903.
[88] H.-L. Cheng, Y.-S. Mai, W.-Y. Chou, L.-R. Chang, X.-W. Liang, *Adv. Funct. Mater.* **2007**, *17*, 3639.
[89] C. C. Yang, S. Li, J. Armellin, *J. Phys. Chem. C* **2007**, *111*, 17512.
[90] D. Knipp, R. A. Street, A. Völkel, J. Ho, *J. Appl. Phys.* **2003**, *93*, 347.
[91] H. L. Cheng, W. Y. Chou, C. W. Kuo, Y. W. Wang, Y. S. Mai, F. C. Tang, S. W. Chu, *Adv. Funct. Mater.* **2008**, *18*, 285.
[92] M. Ando, T. B. Kehoe, M. Yoneya, H. Ishii, M. Kawasaki, C. M. Duffy, T. Minakata, R. T. Phillips, H. Sirringhaus, *Adv. Mater.* **2015**, *27*, 122.
[93] F. Liscio, L. Ferlauto, M. Matta, R. Pfattner, M. Murgia, C. Rovira, M. Mas-Torrent, F. Zerbetto, S. Milita, F. Biscarini, *J. Phys. Chem. C* **2015**, *119*, 15912.
[94] W.-Y. Chou, M.-H. Chang, H.-L. Cheng, Y.-C. Lee, C.-C. Chang, H.-S. Sheu, *J. Phys. Chem. C* **2012**, *116*, 8619.
[95] S. Milita, C. Santato, F. Cicoira, *Appl. Surf. Sci.* **2006**, *252*, 8022.
[96] S. Milita, M. Servidori, F. Cicoira, C. Santato, A. Pifferi, *Nucl. Instrum. Methods Phys. Res. Sect. B Beam Interact. Mater. At.* **2006**, *246*, 101.
[97] A. V. Dzyabchenko, V. E. Zavodnik, V. K. Belsky, *Acta Crystallogr. B* **1979**, *35*, 2250.
[98] Y. Sakamoto, T. Suzuki, M. Kobayashi, Y. Gao, Y. Fukai, Y. Inoue, F. Sato, S. Tokito, *J. Am. Chem. Soc.* **2004**, *126*, 8138.
[99] I. Salzmann, D. Nabok, M. Oehzelt, S. Duhm, A. Moser, G. Heimel, P. Puschnig, C. Ambrosch-Draxl, J. P. Rabe, N. Koch, *Cryst. Growth Des.* **2011**, *11*, 600.
[100] I. Salzmann, S. Duhm, G. Heimel, J. P. Rabe, N. Koch, M. Oehzelt, Y. Sakamoto, T. Suzuki, *Langmuir* **2008**, *24*, 7294.
[101] S. Kowarik, A. Gerlach, A. Hinderhofer, S. Milita, F. Borgatti, F. Zontone, T. Suzuki, F. Biscarini, F. Schreiber, *Phys. Status Solidi RRL* **2008**, *2*, 120.
[102] I. Salzmann, A. Moser, M. Oehzelt, T. Breuer, X. Feng, Z.-Y. Juang, D. Nabok, R. G. Della Valle, S. Duhm, G. Heimel, A. Brillante, E. Venuti, I. Bilotti, C. Christodoulou, J. Frisch, P. Puschnig, C. Draxl, G. Witte, K. Müllen, N. Koch, *ACS Nano* **2012**, *6*, 10874.
[103] J. Stampfl, S. Tasch, G. Leising, U. Scherf, *Synth. Met.* **1995**, *71*, 2125.
[104] R. Resel, *J. Phys. Condens. Matter* **2008**, *20*, 184009.
[105] K. N. Baker, A. V. Fratini, T. Resch, H. C. Knachel, W. W. Adams, E. P. Socci, B. L. Farmer, *Polymer* **1993**, *34*, 1571.
[106] L. Athouel, G. Froyer, M. T. Riou, *Synth. Met.* **1993**, *57*, 4734.
[107] R. Resel, N. Koch, F. Meghdadi, G. Leising, L. Athouel, G. Froyer, F. Hofer, *Cryst. Res. Technol.* **2001**, *36*, 47.
[108] C. Lorch, R. Banerjee, C. Frank, J. Dieterle, A. Hinderhofer, A. Gerlach, F. Schreiber, *J. Phys. Chem. C* **2014**, *119*, 819.
[109] G. Horowitz, B. Bachet, A. Yassar, P. Lang, F. Demanze, J.-L. Fave, F. Garnier, *Chem. Mater.* **1995**, *7*, 1337.
[110] T. Siegrist, R. M. Fleming, R. C. Haddon, R. A. Laudise, A. J. Lovinger, H. E. Katz, P. Bridenbaugh, D. D. Davis, *J. Mater. Res.* **1995**, *10*, 2170.
[111] B. Servet, S. Ries, M. Trotel, P. Alnot, G. Horowitz, F. Garnier, *Adv. Mater.* **1993**, *5*, 461.
[112] B. Servet, G. Horowitz, S. Ries, O. Lagorsse, P. Alnot, A. Yassar, F. Deloffre, P. Srivastava, R. Hajlaoui, *Chem. Mater.* **1994**, *6*, 1809.
[113] A. Moser, I. Salzmann, M. Oehzelt, A. Neuhold, H.-G. Flesch, J. Ivanco, S. Pop, T. Toader, D. R. Zahn, D.-M. Smilgies, R. Resel, *Chem. Phys. Lett.* **2013**, *574*, 55.
[114] M. A. Loi, E. da Como, F. Dinelli, M. Murgia, R. Zamboni, F. Biscarini, M. Muccini, *Nat. Mater.* **2005**, *4*, 81.
[115] B. Wedl, R. Resel, G. Leising, B. Kunert, I. Salzmann, M. Oehzelt, N. Koch, A. Vollmer, S. Duhm, O. Werzer, G. Gbabode, M. Sferrazza, Y. H. Geerts, *RSC Adv.* **2012**, *2*, 4404.
[116] J. Bernstein, *Polymorphism in Molecular Crystals*, Clarendon Press, Oxford, UK **2002**.
[117] O. Werzer, N. Boucher, J. P. de Silva, G. Gbabode, Y. H. Geerts, O. Konovalov, A. Moser, J. Novak, R. Resel, M. Sferrazza, *Langmuir* **2012**, *28*, 8530.
[118] C. Lercher, R. Resel, J.-Y. Balandier, C. Niebel, Y. H. Geerts, M. Sferrazza, G. Gbabode, *J. Cryst. Growth* **2014**, *386*, 128.
[119] C. Lercher, C. Röthel, O. M. Roscioni, Y. H. Geerts, Q. Shen, C. Teichert, R. Fischer, G. Leising, M. Sferrazza, G. Gbabode, R. Resel, *Chem. Phys. Lett.* **2015**, *630*, 12.
[120] M. L. Tang, T. Okamoto, Z. Bao, *J. Am. Chem. Soc.* **2006**, *128*, 16002.
[121] F. Valiyev, W.-S. Hu, H.-Y. Chen, M.-Y. Kuo, I. Chao, Y.-T. Tao, *Chem. Mater.* **2007**, *19*, 3018.
[122] Q. Yuan, S. C. B. Mannsfeld, M. L. Tang, M. F. Toney, J. Lüning, Z. Bao, *J. Am. Chem. Soc.* **2008**, *130*, 3502.
[123] M. A. Heinrich, J. Pflaum, A. K. Tripathi, W. Frey, M. L. Steigerwald, T. Siegrist, *J. Phys. Chem. C* **2007**, *111*, 18878.
[124] A. C. Dürr, F. Schreiber, M. Münch, N. Karl, B. Krause, V. Kruppa, H. Dosch, *Appl. Phys. Lett.* **2002**, *81*, 2276.
[125] S. Kowarik, A. Gerlach, S. Sellner, L. Cavalcanti, O. Konovalov, F. Schreiber, *Appl. Phys. A* **2008**, *95*, 233.
[126] S. Kowarik, A. Gerlach, S. Sellner, F. Schreiber, L. Cavalcanti, O. Konovalov, *Phys. Rev. Lett.* **2006**, *96*, 125504.
[127] T. N. Krauss, E. Barrena, X. N. Zhang, D. G. de Oteyza, J. Major, V. Dehm, F. Würthner, L. P. Cavalcanti, H. Dosch, *Langmuir* **2008**, *24*, 12742.
[128] A. L. Briseno, S. C. B. Mannsfeld, C. Reese, J. M. Hancock, Y. Xiong, S. A. Jenekhe, Z. Bao, Y. Xia, *Nano Lett.* **2007**, *7*, 2847.
[129] R. J. Chesterfield, J. C. McKeen, C. R. Newman, C. D. Frisbie, P. C. Ewbank, K. R. Mann, L. L. Miller, *J. Appl. Phys.* **2004**, *95*, 6396.
[130] F. Liscio, S. Milita, C. Albonetti, P. D' Angelo, A. Guagliardi, N. Masciocchi, R. G. Della Valle, E. Venuti, A. Brillante, F. Biscarini, *Adv. Funct. Mater.* **2012**, *22*, 943.
[131] A. Mänz, T. Breuer, G. Witte, *Cryst. Growth Des.* **2015**, *15*, 395.
[132] H. Wada, D. de Caro, L. Valade, T. Ozawa, Y. Bando, T. Mori, *Thin Solid Films* **2009**, *518*, 299.
[133] G. Sini, J. S. Sears, J.-L. Brédas, *J. Chem. Theory Comput.* **2011**, *7*, 602.
[134] R. P. Shibaeva, V. P. Kaminskii, E. B. Yagubskii, *Mol. Cryst. Liq. Cryst.* **1985**, *119*, 361.

[135] K. Kawabata, K. Shimotani, T. Sambongi, *J. Korean Phys. Soc.* **1997**, *31*, 431.
[136] K. Bechgaard, T. J. Kistenmacher, A. N. Bloch, D. O. Cowan, *Acta Crystallogr. B* **1977**, *33*, 417.
[137] T. J. Kistenmacher, T. J. Emge, A. N. Bloch, D. O. Cowan, *Acta Crystallogr. B* **1982**, *38*, 1193.
[138] D. Vermeulen, L. Y. Zhu, K. P. Goetz, P. Hu, H. Jiang, C. S. Day, O. D. Jurchescu, V. Coropceanu, C. Kloc, L. E. McNeil, *J. Phys. Chem. C* **2014**, *118*, 24688.
[139] K. P. Goetz, D. Vermeulen, M. E. Payne, C. Kloc, L. E. McNeil, O. D. Jurchescu, *J. Mater. Chem. C* **2014**, *2*, 3065.
[140] F. Paulus, B. D. Lindner, H. Reiß, F. Rominger, A. Leineweber, Y. Vaynzof, H. Sirringhaus, U. H. F. Bunz, *J. Mater. Chem. C* **2015**, *3*, 1604.
[141] H. Ebata, T. Izawa, E. Miyazaki, K. Takimiya, M. Ikeda, H. Kuwabara, T. Yui, *J. Am. Chem. Soc.* **2007**, *129*, 15732.
[142] Y. Yuan, G. Giri, A. L. Ayzner, A. P. Zoombelt, S. C. B. Mannsfeld, J. Chen, D. Nordlund, M. F. Toney, J. Huang, Z. Bao, *Nat. Commun.* **2014**, *5*, 3005.
[143] A. O. F. Jones, Y. H. Geerts, J. Karpinska, A. R. Kennedy, R. Resel, C. Röthel, C. Ruzié, O. Werzer, M. Sferrazza, *ACS Appl. Mater. Interfaces* **2015**, *7*, 1868.
[144] T. Izawa, E. Miyazaki, K. Takimiya, *Adv. Mater.* **2008**, *20*, 3388.
[145] M. J. Kang, T. Yamamoto, S. Shinamura, E. Miyazaki, K. Takimiya, *Chem. Sci.* **2010**, *1*, 179.
[146] T. Yamamoto, S. Shinamura, E. Miyazaki, K. Takimiya, *Bull. Chem. Soc. Jpn.* **2010**, *83*, 120.
[147] P. Beyer, T. Breuer, S. Ndiaye, A. Zykov, A. Viertel, M. Gensler, J. P. Rabe, S. Hecht, G. Witte, S. Kowarik, *ACS Appl. Mater. Interfaces* **2014**, *6*, 21484.
[148] A. M. Hiszpanski, R. M. Baur, B. Kim, N. J. Tremblay, C. Nuckolls, A. R. Woll, Y.-L. Loo, *J. Am. Chem. Soc.* **2014**, *136*, 15749.
[149] S. Pankaj, D. Enke, M. Steinhart, M. Beiner, G. T. Rengarajan, *Nano Lett.* **2007**, *7*, 1381.
[150] M.-A. Perrin, M. A. Neumann, H. Elmaleh, L. Zaske, *Chem. Commun.* **2009**, 3181.
[151] G. T. Rengarajan, D. Enke, M. Steinhart, M. Beiner, *Phys. Chem. Chem. Phys.* **2011**, *13*, 21367.
[152] J. D. Yeager, K. J. Ramos, N. H. Mack, H.-L. Wang, D. E. Hooks, *Cryst. Growth Des.* **2012**, *12*, 5513.
[153] H. M. A. Ehmann, O. Werzer, *Cryst. Growth Des.* **2014**, *14*, 3680.
[154] D. Reischl, C. Röthel, P. Christian, E. Roblegg, H. M. A. Ehmann, I. Salzmann, O. Werzer, *Cryst. Growth Des.* **2015**, *15*, 4687.
[155] S. T. Salammal, J.-Y. Balandier, J.-B. Arlin, Y. Olivier, V. Lemaur, L. Wang, D. Beljonne, J. Cornil, A. R. Kennedy, Y. H. Geerts, B. Chattopadhyay, *J. Phys. Chem. C* **2014**, *118*, 657.
[156] T. Rasing, I. Muševič, *Surfaces and Interfaces of Liquid Crystals*, Springer Berlin Heidelberg, Germany **2004**.
[157] G. Barbero, L. R. Evangelista, *Liq. Cryst. Rev.* **2014**, *2*, 72.
[158] W. Pisula, Ž. Tomovič, B. El Hamaoui, M. D. Watson, T. Pakula, K. Müllen, *Adv. Funct. Mater.* **2005**, *15*, 893.
[159] E. Pouzet, V. D. Cupere, C. Heintz, J. W. Andreasen, D. W. Breiby, M. M. Nielsen, P. Viville, R. Lazzaroni, G. Gbabode, Y. H. Geerts, *J. Phys. Chem. C* **2009**, *113*, 14398.
[160] E. Grelet, S. Dardel, H. Bock, M. Goldmann, E. Lacaze, F. Nallet, *Eur. Phys. J. E* **2010**, *31*, 343.
[161] I. Cour, Z. Pan, L. T. Lebruin, M. A. Case, M. Furis, R. L. Headrick, *Org. Electron.* **2012**, *13*, 419.
[162] J. Tant, Y. H. Geerts, M. Lehmann, V. De Cupere, G. Zucchi, B. W. Laursen, T. Bjørnholm, V. Lemaur, V. Marcq, A. Burquel, E. Hennebicq, F. Gardebien, P. Viville, D. Beljonne, R. Lazzaroni, J. Cornil, *J. Phys. Chem. B* **2005**, *109*, 20315.
[163] G. Gbabode, N. Dumont, F. Quist, G. Schweicher, A. Moser, P. Viville, R. Lazzaroni, Y. H. Geerts, *Adv. Mater.* **2012**, *24*, 658.
[164] B. Chattopadhyay, C. Ruzié, R. Resel, Y. H. Geerts, *Liq. Cryst.* **2014**, *41*, 302.
[165] R. A. Cormier, B. A. Gregg, *J. Phys. Chem. B* **1997**, *101*, 11004.
[166] N. A. Minder, S. Ono, Z. Chen, A. Facchetti, A. F. Morpurgo, *Adv. Mater.* **2012**, *24*, 503.
[167] G. Schweicher, Y. Olivier, V. Lemaur, Y. H. Geerts, *Isr. J. Chem.* **2014**, *54*, 595.
[168] C. Wang, H. Dong, W. Hu, Y. Liu, D. Zhu, *Chem. Rev.* **2012**, *112*, 2208.
[169] J. Mei, Y. Diao, A. L. Appleton, L. Fang, Z. Bao, *J. Am. Chem. Soc.* **2013**, *135*, 6724.
[170] B. Stadlober, V. Satzinger, H. Maresch, D. Somitsch, A. Haase, H. Pichler, W. Rom, G. Jakopic, in *Proc SPIE 5217 Org. Field Eff. Transistors II* (Ed.: C. D. Dimitrakopoulos), SPIE, Bellingham, WA, USA **2003**, pp. 112.
[171] A. Troisi, G. Orlandi, *J. Phys. Chem. B* **2005**, *109*, 1849.
[172] W. H. Taylor, *Z. Krist.* **1936**, *93*, 151.
[173] S. A. Akopyan, R. L. Avoyan, Y. T. Struchkov, *Z. Strukt. Khim.* **1962**, *3*, 602.
[174] D. E. Henn, W. G. Williams, D. J. Gibbons, *J. Appl. Crystallogr.* **1971**, *4*, 256.
[175] I. Bulgarovskaya, V. Vozzhennikov, S. Aleksandrov, V. Belsky, *Latv. PSR Zinat. Akad. Vestis, Fiz. Teh. Zinat.* **1983**, *4*, 53.
[176] O. D. Jurchescu, A. Meetsma, T. T. M. Palstra, *Acta Crystallogr. B* **2006**, *62*, 330.
[177] E. Menard, V. Podzorov, S.-H. Hur, A. Gaur, M. E. Gershenson, J. A. Rogers, *Adv. Mater.* **2004**, *16*, 2097.
[178] J. Takeya, M. Yamagishi, Y. Tominari, R. Hirahara, Y. Nakazawa, T. Nishikawa, T. Kawase, T. Shimoda, S. Ogawa, *Appl. Phys. Lett.* **2007**, *90*, 102120.
[179] A. Yassar, *Polym. Sci. Ser. C* **2014**, *56*, 4.
[180] V. R. Hathwar, M. Sist, M. R. V. Jørgensen, A. H. Mamakhel, X. Wang, C. M. Hoffmann, K. Sugimoto, J. Overgaard, B. B. Iversen, *IUCrJ* **2015**, *2*, 563.
[181] T. Matsukawa, M. Yoshimura, M. Uchiyama, M. Yamagishi, A. Nakao, Y. Takahashi, J. Takeya, Y. Kitaoka, Y. Mori, T. Sasaki, *Jpn. J. Appl. Phys.* **2010**, *49*, 085502.
[182] T. Matsukawa, M. Yoshimura, K. Sasai, M. Uchiyama, M. Yamagishi, Y. Tominari, Y. Takahashi, J. Takeya, Y. Kitaoka, Y. Mori, T. Sasaki, *J. Cryst. Growth* **2010**, *312*, 310.
[183] J. Chen, J. Anthony, D. C. Martin, *J. Phys. Chem. B* **2006**, *110*, 16397.
[184] G. Giri, E. Verploegen, S. C. B. Mannsfeld, S. Atahan-Evrenk, D. H. Kim, S. Y. Lee, H. A. Becerril, A. Aspuru-Guzik, M. F. Toney, Z. Bao, *Nature* **2011**, *480*, 504.
[185] G. Giri, R. Li, D.-M. Smilgies, E. Q. Li, Y. Diao, K. M. Lenn, M. Chiu, D. W. Lin, R. Allen, J. Reinspach, S. C. B. Mannsfeld, S. T. Thoroddsen, P. Clancy, Z. Bao, A. Amassian, *Nat. Commun.* **2014**, *5*, 3573.
[186] Y. Diao, B. C.-K. Tee, G. Giri, J. Xu, D. H. Kim, H. A. Becerril, R. M. Stoltenberg, T. H. Lee, G. Xue, S. C. B. Mannsfeld, Z. Bao, *Nat. Mater.* **2013**, *12*, 665.
[187] Y. Diao, K. M. Lenn, W.-Y. Lee, M. A. Blood-Forsythe, J. Xu, Y. Mao, Y. Kim, J. A. Reinspach, S. Park, A. Aspuru-Guzik, G. Xue, P. Clancy, Z. Bao, S. C. B. Mannsfeld, *J. Am. Chem. Soc.* **2014**, *136*, 17046.
[188] J. Chen, M. Shao, K. Xiao, A. J. Rondinone, Y.-L. Loo, P. R. C. Kent, B. G. Sumpter, D. Li, J. K. Keum, P. J. Diemer, J. E. Anthony, O. D. Jurchescu, J. Huang, *Nanoscale* **2014**, *6*, 449.
[189] O. Jurchescu, D. Mourey, S. Subramanian, S. Parkin, B. Vogel, J. Anthony, T. Jackson, D. Gundlach, *Phys. Rev. B* **2009**, *80*, 085201.
[190] R. Li, J. W. Ward, D.-M. Smilgies, M. M. Payne, J. E. Anthony, O. D. Jurchescu, A. Amassian, *Adv. Mater.* **2012**, *24*, 5553.
[191] J. Y. Kim, T. Yasuda, Y. S. Yang, N. Matsumoto, C. Adachi, *Chem. Commun.* **2014**, *50*, 1523.

[192] L. Yu, *Acc. Chem. Res.* **2010**, *43*, 1257.
[193] J. Bernstein, R. J. Davey, J.-O. Henck, *Angew. Chem. Int. Ed.* **1999**, *38*, 3440.
[194] D. Erdemir, A. Y. Lee, A. S. Myerson, *Acc. Chem. Res.* **2009**, *42*, 621.
[195] K. A. Jackson, *Ind. Eng. Chem.* **1965**, *57*, 28.
[196] F.-J. Meyer zu Heringdorf, M. C. Reuter, R. M. Tromp, *Nature* **2001**, *412*, 517.
[197] F. Biscarini, R. Zamboni, P. Samorí, P. Ostoja, C. Taliani, *Phys. Rev. B* **1995**, *52*, 14868.
[198] F. Biscarini, P. Samorí, O. Greco, R. Zamboni, *Phys. Rev. Lett.* **1997**, *78*, 2389.
[199] S. Verlaak, S. Steudel, P. Heremans, D. Janssen, M. S. Deleuze, *Phys. Rev. B* **2003**, *68*, 195409.
[200] A. Al-Mahboob, Y. Fujikawa, T. Sakurai, J. T. Sadowski, *Adv. Funct. Mater.* **2013**, *23*, 2653.
[201] H. Liu, P. Reinke, *J. Chem. Phys.* **2006**, *124*, 164707.
[202] S. Bommel, N. Kleppmann, C. Weber, H. Spranger, P. Schäfer, J. Novak, S. V. Roth, F. Schreiber, S. H. L. Klapp, S. Kowarik, *Nat. Commun.* **2014**, *5*, 5388.
[203] A. Al-Mahboob, Y. Fujikawa, J. T. Sadowski, T. Hashizume, T. Sakurai, *Phys. Rev. B* **2010**, *82*, 235421.
[204] T. A. Witten, L. M. Sander, *Phys. Rev. Lett.* **1981**, *47*, 1400.
[205] R. Ruiz, B. Nickel, N. Koch, L. C. Feldman, R. F. Haglund, A. Kahn, F. Family, G. Scoles, *Phys. Rev. Lett.* **2003**, *91*, 136102.
[206] R. Ruiz, D. Choudhary, B. Nickel, T. Toccoli, K.-C. Chang, A. C. Mayer, P. Clancy, J. M. Blakely, R. L. Headrick, S. Iannotta, G. G. Malliaras, *Chem. Mater.* **2004**, *16*, 4497.
[207] C. Ambrosch-Draxl, D. Nabok, P. Puschnig, C. Meisenbichler, *New J. Phys.* **2009**, *11*, 125010.
[208] A. C. Mayer, A. Kazimirov, G. G. Malliaras, *Phys. Rev. Lett.* **2006**, *97*, 105503.
[209] C. Di, G. Yu, Y. Liu, Y. Guo, X. Sun, J. Zheng, Y. Wen, Y. Wang, W. Wu, D. Zhu, *Phys. Chem. Chem. Phys.* **2009**, *11*, 7268.
[210] G. Gbabode, B. Chattopadhyay, in *Non-Equilib. Phenom. Confin. Soft Matter* (Ed.: S. Napolitano), Springer International Publishing, Switzerland **2015**.
[211] W. C. Marra, P. Eisenberger, A. Y. Cho, *J. Appl. Phys.* **1979**, *50*, 6927.
[212] M. Yoneya, M. Kawasaki, M. Ando, *J. Phys. Chem. C* **2012**, *116*, 791.
[213] D. He, Y. Zhang, Q. Wu, R. Xu, H. Nan, J. Liu, J. Yao, Z. Wang, S. Yuan, Y. Li, Y. Shi, J. Wang, Z. Ni, L. He, F. Miao, F. Song, H. Xu, K. Watanabe, T. Taniguchi, J.-B. Xu, X. Wang, *Nat. Commun.* **2014**, *5*, 5162.
[214] A. Virkar, S. C. B. Mannsfeld, J. H. Oh, M. F. Toney, Y. H. Tan, G. Liu, J. C. Scott, R. Miller, Z. Bao, *Adv. Funct. Mater.* **2009**, *19*, 1962.
[215] O. Werzer, B. Stadlober, A. Haase, H.-G. Flesch, R. Resel, *Eur. Phys. J. – Appl. Phys.* **2009**, *46*, 20403.
[216] M. Dohr, O. Werzer, Q. Shen, I. Salzmann, C. Teichert, C. Ruzié, G. Schweicher, Y. H. Geerts, M. Sferrazza, R. Resel, *ChemPhysChem* **2013**, *14*, 2554.
[217] M.-C. Jung, M. R. Leyden, G. O. Nikiforov, M. V. Lee, H.-K. Lee, T. J. Shin, K. Takimiya, Y. Qi, *ACS Appl. Mater. Interfaces* **2014**, *7*, 1833.
[218] A. Brillante, I. Bilotti, R. G. Della Valle, E. Venuti, A. Girlando, M. Masino, F. Liscio, S. Milita, C. Albonetti, P. D'angelo, A. Shehu, F. Biscarini, *Phys. Rev. B* **2012**, *85*, 195308.
[219] L. Viani, C. Risko, M. F. Toney, D. W. Breiby, J.-L. Brédas, *ACS Nano* **2013**, *8*, 690.
[220] C. A. Mitchell, L. Yu, M. D. Ward, *J. Am. Chem. Soc.* **2001**, *123*, 10830.
[221] F. Liscio, C. Albonetti, K. Broch, A. Shehu, S. D. Quiroga, L. Ferlauto, C. Frank, S. Kowarik, R. Nervo, A. Gerlach, S. Milita, F. Schreiber, F. Biscarini, *ACS Nano* **2013**, *7*, 1257.
[222] A. J. Page, R. P. Sear, *J. Am. Chem. Soc.* **2009**, *131*, 17550.
[223] Y. Diao, T. Harada, A. S. Myerson, T. Alan Hatton, B. L. Trout, *Nat. Mater.* **2011**, *10*, 867.
[224] C. Lorch, R. Banerjee, C. Frank, J. Dieterle, A. Hinderhofer, A. Gerlach, F. Schreiber, *J. Phys. Chem. C* **2015**, *119*, 819.
[225] D.-M. Smilgies, R. Li, G. Giri, K. W. Chou, Y. Diao, Z. Bao, A. Amassian, *Phys. Status Solidi RRL* **2013**, *7*, 177.
[226] C. D. Liman, S. Choi, D. W. Breiby, J. E. Cochran, M. F. Toney, E. J. Kramer, M. L. Chabinyc, *J. Phys. Chem. B* **2013**, *117*, 14557.
[227] R. Thakuria, M. D. Eddleston, E. H. H. Chow, G. O. Lloyd, B. J. Aldous, J. F. Krzyzaniak, A. D. Bond, W. Jones, *Angew. Chem. Int. Ed.* **2013**, *52*, 10541.
[228] A. I. Lupulescu, J. D. Rimer, *Science* **2014**, *344*, 729.
[229] S. L. Price, *Chem. Soc. Rev.* **2014**, *43*, 2098.